Re-deployment of germ layers related TFs shows regionalized expression during two non-embryonic developments

Ricci Lorenzo, Fabien Cabrera, Sonia Lotito, Stefano Tiozzo

Re-deployment of germ layers related TFs shows regionalized expression during two non-embryonic developments

Ricci Lorenzo, Fabien Cabrera, Sonia Lotito, Stefano Tiozzo

www.elsevier.com/locate/developmentalbiology

PII: S0012-1606(15)30268-2
DOI: http://dx.doi.org/10.1016/j.ydbio.2016.05.016
Reference: YDBIO7123

To appear in: *Developmental Biology*

Received date: 2 November 2015
Revised date: 11 May 2016
Accepted date: 12 May 2016

Cite this article as: Ricci Lorenzo, Fabien Cabrera, Sonia Lotito and Stefan Tiozzo, Re-deployment of germ layers related TFs shows regionalized expression during two non-embryonic developments, *Developmental Biology* http://dx.doi.org/10.1016/j.ydbio.2016.05.016

Re-deployment of germ layers related TFs shows regionalized expression during two non-embryonic developments

Ricci Lorenzo[1], Fabien Cabrera[1], Sonia Lotito[1], Stefano Tiozzo[1*]

[1]Sorbonne Universités, UPMC Univ. Paris 06, CNRS, Laboratoire de Biologie du Développement de Villefranche-sur-mer (LBDV), 06230 Villefranche sur-mer, France

[*]Corresponding author.

Abstract

In all non-vertebrate metazoan phyla, species that evolved non-embryonic developmental pathways as means of propagation or regeneration can be found. In this context, new bodies arise through asexual reproduction processes (such as budding) or whole body regeneration, that lack the familiar temporal and spatial cues classically associated with embryogenesis, like maternal determinants, or gastrulation. The molecular mechanisms underlying those non-embryonic developments (i.e., regeneration and asexual reproduction), and their relationship to those deployed during embryogenesis are poorly understood. We have addressed this question in the colonial ascidian *Botryllus schlosseri*, which undergoes an asexual reproductive process via palleal budding (PB), as well as a whole body regeneration by vascular budding (VB). We identified early regenerative structures during VB and then followed the fate of differentiating tissues during both non-embryonic developments (PB and VB) by monitoring the expression of genes known to play key functions in germ layer specification with well conserved expression patterns in solitary ascidian embryogenesis. The expression patterns of *FoxA1, GATAa, GATAb, Otx, Bra, Gsc* and *Tbx2/3* were analyzed during both PB and VB. We found that the majority of these transcription factors were expressed during both non-embryonic developmental processes, revealing a regionalization of the palleal and vascular buds. Knockdown of *GATAa* by siRNA in palleal buds confirmed that

preventing the correct development of one of these regions blocks further tissue specification. Our results indicate that during both normal and injury-induced budding, a similar alternative developmental program operates via early commitment of epithelial regions.

Introduction

How cells acquire the competence to form specific lineages along the course of embryogenesis is a central theme in developmental biology. For instance, gastrulation, and the resulting division into two or three germ layers, represents a developmental switch point, at the end of which, through the distribution of maternal determinants or by means of intercellular interactions, most of the future adult cell lineages are specified. In triploblastic bilaterians, the lineages derived from the ecto-, meso- and endo-derms are not always sharply defined, nor perfectly conserved (Le Douarin and Dupin, 2012; Weston and Thiery, 2015). While the homology of the germ layers and their derived tissues is still not clear within eumetazoans (Martindale et al., 2004), extensive comparative studies across different phyla show that eumetazoan embryogenesis share some conserved gene expression patterns and relatively robust gene regulatory networks (GRN) (Beby and Lamonerie, 2013; Brown et al., 2014; Erwin, 2009; Naiche et al., 2005; Showell et al., 2004; Wardle and Papaioannou, 2008). Despite the fact that interactions among such TFs are not always conserved (Brown et al., 2014; Doglio et al., 2013), their expression patterns are often consistent among multiple phyla and can be tentatively used as markers of the three germ layers. In particular, ascidians are excellent models for embryology due to robust, rapid development and little variation in morphology, cleavage patterns, and cell fate specification across the different species studied (Chabry, 1887; Conklin, 1905; Kumano and Nishida, 2007; Lemaire, 2009, 2011; Lemaire et al., 2008). Solitary ascidian species have been extensively used as models to dissect GRNs

(Imai et al., 2009; Oda-Ishii et al., 2005; Stolfi et al., 2014), the functions of developmental genes (Hudson and Lemaire, 2001; Wada et al., 2004) and cell fate specification mechanisms (Dumollard et al., 2013; Haupaix et al., 2013).

A subset of ascidian species is colonial. Whereas less studied, the embryogenesis of colonial species is comparable to that of solitary ascidians in terms of cleavage patterns, gastrulation and morphogenesis (Brown and Swalla, 2012; Satoh, 1994; supp. video V1, V2). Based on these anatomical characteristics the embryogenesis of solitary species is used as proxy for the one of colonial species (Hirano and Nishida, 2000; Kumano et al., 2006; Kumano et al., 2014; Ogasawara et al., 1996; Wada et al., 1996; Wada et al., 2004). In addition, colonial species can propagate asexually, via a budding process during which, new adults (zooids) are generated *de novo*, such that an adult colony consists of a group of physically connected and genetically identical zooids (Berrill, 1941; Berrill, 1948; Berrill, 1951; Milkman, 1967; Watanabe and Newberry, 1976; Nakauchi and Kawamura, 1978). This process is called blastogenesis, and proceeds by stereotyped ontogenetic stages (Izzard, 1973; Lauzon et al., 2002). In addition to blastogenesis, new bodies can also be generated in another non-embryonic developmental process called vascular budding, which in some species occurs concurrently with blastogenesis, and in others is a regenerative response to injury (Kürn et al., 2011; Nakauchi, 1982). In both non-embryonic developments, the new zooids originate from a poorly characterized subset of cells of the existing adult zooid, either mobile precursors or regions of epithelia, which form structures called buds. Buds develop as these regions proliferate, undergo a series of epithelial folding and following organogenesis finally lead to a functional adult body (Stolfi and Brown, 2015). These non-embryonic developments have striking differences to embryogenesis, chiefly they lack the distribution of maternal determinants, suggesting a regulative rather than a mosaic nature of development, and their

ontogenesis, that follows different anatomical steps (Brown and Swalla, 2012; Kürn et al., 2011).

In the colonial ascidian *Botryllus schlosseri*, the study of embryogenesis is limited by the small number of eggs carried by each zooid (Gasparini et al., 2015; Milkman, 1967), by the internal brooding of embryos (Sabbadin and Zaniolo, 1979; Zaniolo et al., 1986) and by the presence of a pseudo placenta and a particular thick chorion that makes *in situ* hybridization particularly difficult (Manni et al., 1993; Manni et al., 1994; Tiozzo et al., 2005). Conversely, in *Botryllus* colonies, growth is ensured by asexual reproduction, i.e. blastogenesis, which occurs through a process termed palleal budding (PB)(Berrill, 1941; Izzard, 1973; Manni et al., 2007; Manni et al., 2014; Milkman, 1967; Sabbadin et al., 1975) where buds arise from specific regions in the peribranchial epithelium of the parental zooid (Fig. 1A-C), and develop in a stereotyped fashion (Fig. 1C, Lauzon et al., 2002; Manni et al., 2014). A *Botryllus* colony consists of three coexisting asexual generations: the adult filtering zooids, their buds, called primary buds, and the secondary buds (or budlets), sprouting from the primary buds (Fig. 1). The development of primary buds and budlets is continuous and highly synchronized. During the phase named take-over, all the adult zooids get resorbed through a coordinated phase of apoptosis, and are replaced by primary buds, while budlets become primary buds and give rise to new budlets (Lauzon et al., 2002; Manni et al., 2014). Briefly, formation of a new body is initiated at each blastogenetic cycle transition (Fig. 1C). The new budlet appears as a disc of thickened cells (stage A1), forms in specific region of a primary bud peribranchial epithelium (see Fig. 1C, also for following budlet descriptions). The budlet grows and arches anteriorly, respectively to its parental bud (stage A2/B1), then forms a transient, double vesicle (stage B2). In following stages, epithelial folds re-organize the budlet (stage C1), and lead to a compartmentalized structure (stage C2). During C1 and C2 stages, epithelial outgrowths start forming the heart, gut and neural complex rudiments. In stage D, the budlet rotates and adopts

the same orientation as the primary buds and zooids. From this point on, its global morphology is very similar to the adult, however, organogenesis and growth will continue until the zooid stage. The life of a body lasts as long as three successive blastogenetic cycles (about three weeks at 18°C), one as budlet, the second as primary bud, and the third and last cycle as an adult zooid. Each step of the cycle can be characterized based on visual morphological landmarks.

In addition to PB, *B. schlosseri*, can regenerate a whole zooid by an injury-triggered process of vascular budding (VB). When all zooids and buds are removed from the colony (Fig. 5 A-C), the vascular bud originates in niches along the peripheral vascular system through clusters of cells that forms a hollow vesicle (Fig. 5 D-G). From this point on the epithelia proliferate and fold in a non-stereotyped way leading to the formation of abnormal, non-functional zooids (Fig. S10; Sabbadin et al., 1975; Voskoboynik et al., 2007). Only after several cycles of blastogenesis the zooid regains normal developmental patterns (Milkman and Byrne, 1961; Brown et al., 2009; Sabbadin et al., 1975; Voskoboynik et al., 2007).

Whereas PB and VB lead to the same adult body plan, these two non-embryonic developments show striking differences from one another: PB is stereotyped and is part of the life history of the colony, whereas VB is triggered by injury and reaches the zooid form after an irregular, non-stereotyped morphogenesis (Sabbadin et al., 1975; Voskoboynik et al., 2007). In addition, whereas palleal buds forms in a defined region of the peribranchial epithelia (Manni et al., 2014), the cellular origin of VB is still unresolved and it could be attributed to a population of multi/pluripotent haemoblasts, with the involvement of the vascular epithelia, or through the contribution of both blood and vessels (Rinkevich et al., 1995; Sabbadin et al., 1975).

With the long term goal of better understand how a similar body plan can emerge from different biological contexts we characterised seven key TFs chosen for their conserved role in ascidian and, more generally, in bilaterian germ layer specification and expressed in germ layer derivatives (Arceci et al., 1993; Boyle and Seaver, 2010; Di Gregorio et al., 2001; Gillis et al., 2007; Horikawa et al., 2013; Hudson and Lemaire, 2001; José-Edwards et al., 2013; Lemaire and Gurdon, 1994; Papaioannou, 2014; Patient and McGhee, 2002; Roure et al., 2014; Yasuo and Lemaire, 2001).

We analysed the pattern of expression of *GATAb* and *Otx* (ectoderm), *Goosecoid* (*Gsc*), *Brachyury (Bra)* and *Tbx2/3* (mesoderm) and *Fox-A1* and *GATA*a (endoderm) during both PB and VB. We also tested the function of one key TF using siRNA knock down. Here we report and discuss how a subset of these genes are re-deployed in two non-embryonic developmental pathways and assess their role in regionalizing early palleal and vascular buds, suggesting that non-embryonic developments include a phase of tissue specification, cell type diversification and spatial rearrangement that may be compared to the drastic cellular and structural changes that occur during the embryo gastrulation.

Materials and Methods

Animals

Colonies of *Botryllus schlosseri* were raised on glass slides in a mariculture system as described previously (Langenbacher et al., 2015). Palleal bud development was staged according to the Lauzon staging method (Lauzon et al., 2002).

Induction of vascular budding

Colonies of *B.schlosseri* at stage D were dissected using microsurgery tools and syringe needles (30G, Terumo, SG2-3013) under a stereomicroscope. After removal of all zooids and

buds, animals were cleaned and allowed to regenerate in filtered sea water (FSW), in small containers (<1L) at 19°C. Water was changed every two days and vascular bud detection performed by daily inspection under a stereomicroscope.

Immunostaining

Immunohistochemistry was performed on regenerating colonies in order to characterize developmental stages during VB. Animals were fixed prior of after live detection of vascular buds using 4% PFA in FSW or 1X Phosphate Buffer Saline (PBS) overnight with agitation at 4°C. Following several washes in PBS, samples were incubated overnight with agitation at 4°C with 1µM TRITC-phalloidin (Sigma-Aldrich, #P1951) in 1X PBS for F-actin staining. Following extensive washes in PBS, samples were incubated at room temperature with Hoechst 33342, 1µg/ml in 1X PBS for 2 hours then mounted in glycerol for microscopy, and imaging was performed with a confocal Leica TCS SP5 microscope. Immunolabeling of tyrosine tubulin was performed in regenerating colony, fixed as described above, after blocking by 5% goat serum in 1X PBS + 0.5% triton, with monoclonal primary antibody, mouse anti-tubulin, tyrosine (Sigma-Aldrich, #T9028), at the dilution of 1:500. Following 2 to 4 days of incubation, at 4°C with agitation, samples were washed in 1X PBS and incubated 2 days with secondary antibody, Alexa Fluor® 488 AffiniPure Goat Anti-Mouse IgG (H+L) (Jackson ImmunoResearch, #115-545-003), diluted 1:200, in 1X PBS +0.1% triton. After extensive PBS washes, samples were counterstained with Hoechst 33342, 1µg/ml in 1X PBS for 2 hours, and their vascular system was screened with a confocal Leica TCS SP5 microscope in order to detect vascular buds.

Gene identification and molecular phylogeny

Candidate genes homologs were retrieved by tblastn, from a *B. schlosseri* transcriptomic database (http://octopus.obs-vlfr.fr/public/botryllus/blast_botryllus.php), using ascidian

(*Ciona sp.* and *Halocynthia roretzi*, when available) or vertebrates' proteins sequences as queries. Accession numbers are listed in Table S1. One *Botryllus* ortholog was found for both *Gsc* and *Otx* genes, two *GATA* TFs, seven *T-BOX (Tbx)* genes and 18 *Fox* genes. Complete ORFs were available for all the studied genes, except *Brachyury*, where the N-terminal side of the predicted protein, containing the T-BOX domain, is incomplete.

For phylogenetic analyses, amino acid sequences were retrieved from Aniseed (http://www.aniseed.cnrs.fr/), Uniprot and Genbank. For each candidate gene, except for Fox and GATA families, amino-acid sequences were aligned with MUSCLE v. 3.7 (Edgar, 2004) and non-conserved domains were removed with TrimAL v. 1.3, using strict trimming parameter (Capella-Gutiérrez et al., 2009). In the case of Fox and GATA genes, large metazoan sequences datasets were graciously shared by Dr. Lapébie and Dr. Gillis, respectively (Gillis et al., 2008; Lapébie et al., 2014). Using a Bayesian computational method, molecular phylogenetic trees were then built and analysed with the BEAUTi and BEAST software package v. 1.8 (Drummond et al., 2012), using the default parameters. Trees were then visualised and annotated with FigTree v. 1.4.2 (http://tree.bio.ed.ac.uk/software/figtree/) (Fig. S1 to S5). The BEAST output files containing all the generated trees, along with the accession numbers of the sequences used for the molecular phylogeny analysis are available upon request. Bayesian phylogenetic analysis statistically supported the orthology of *Botryllus* sequences with other ascidians. The topology of the trees globally reflected metazoan relationships according to recent phylogenetic analyses (Delsuc et al., 2006), except in the case of GATA genes, where ascidian *GATAa* sequences were found to group with to those of protostomes than deuterostomes (Fig. S1).

Fluorescent in situ hybridization (FISH)

For each gene, couples of forward and reverse primers were designed in order to obtain amplified fragments between 700 and 1200 bp. Animals were anesthetised by addition of MS-222 (Sigma-Aldrich, E10521) in FSW. FISH was conducted as previously described (Langenbacher et al., 2015), with the following modifications: no proteinase K digestion and subsequent post-fixation were performed; hybridization time was extended up to 72hrs, keeping the sample in constant agitation at 58°C; and incubation with HRP-conjugated anti-digoxigenin antibody (Roche, 11207733910) was extended to 72hrs. DIG-probe detection was performed by 2hr incubation (at room temperature, with agitation, in the dark) in a 0.25 mg/ml bench-made FITC-tyramide stock solution (Zhou and Vize, 2004) diluted 1 in 100 (v/v) in 1X PBS, with 0.001% H_2O_2. Counterstaining was performed with Hoechst 33342 (10 µg/ml in 1X PBS) before mounting in glycerol and imaging with a confocal Leica TCS SP5 microscope. Primers sequences used for FISH and KD experiments are given in Table S2. For each gene between 5 and 15 FISH have been performed, for each experiment all the PB and VB stages have been analysed. For PB, 10 to 20 zooids and buds have been screened for each stage. The patterns of expression described have been detected in all the samples screened. A mix of genotypes has been used in order to ascertain the consistency of gene expression.

siRNA Knock-down (KD)

For *GATAa*, a pair of primers was synthesised to amplify 700-1200 bp DNA fragments. To test the specificity of *GATAa* siRNA treatment, siRNA designed on GFP has been used as control and did not show any noticeable phenotype (Laird et al., 2005; Nyholm et al., 2006; Tiozzo and De Tomaso, 2009; Tiozzo et al., 2008b). Long dsRNA was synthetized with the T7 RiboMAX™ Express Large Scale RNA Production System (Promega, P1320). Long dsRNA were purified by salt and alcohol precipitation and digested with the ShortCut® RNase III kit (NEB, M0245L) to produce small interfering dsRNA (siRNA) of 18-21 bp. Prior KD experiments, colonies of *B.schlosseri* were sub-cloned and grown on different glass

slides in order to obtain genetically identical clones at the same developmental stage. Purified siRNAs were then delivered daily as previously described (Tiozzo et al., 2008b) both by injection in the peripheral vasculature (1µl at 50 µM) and by 3 hours incubation (100 pmol in 500 µl of FSW). Animals were fed and maintained at 19°C in a large volume of clean SW between two siRNA administrations. The whole treatment lasted between 4 and 7 days. A negative control was performed on a colony of the same size, stage and genotype as the KD colony. KD efficiency was estimated qualitatively by FISH. Gene KD impact on the development was also evaluated by morphological observations, both on live and fixed animals. The latter were fixed O/N in 4% PFA FSW then washed in 1X PBS before f-actin and nuclei staining with TRITC-phalloidin, 1µM in 1X PBS, (Sigma-Aldrich, P1951) and Hoechst 33342, 1µg/ml in 1X PBS. Imaging was performed with a confocal Leica TCS SP5 microscope. The KD has been repeated in n=6 different genotypes, in each case, the colony was cut into three to four pieces of 4-5 zooids each (and attached buds) for FISH and histology, respectively.

Results

Pattern of expression of ectoderm-associated TFs during PB

In order to understand how different ectodermal fates are specified during PB, we followed the expression of two genes involved in patterning the main ectodermally derived tissues, in chordate embryogenesis (Hinman et al., 2000; Read et al., 1998; Rhinn et al., 1999; Sheng and Stern, 1999). We assessed expression of the *Botryllus* orthologs of *GATAb* and *Otx* at each stage of PB. In solitary ascidians *H. roretzi* and *C. intestinalis*, *Otx* has been reported as a main actor for induction of anterior neural fate, and is found expressed not only in the embryo neural precursors but also within the surrounding endoderm (Hudson and Lemaire,

2001; Imai et al., 2002; Wada et al., 2004). Conversely, *GATAb* expression has only been poorly characterized in ascidian embryos, where it has been reported expressed along embryogenesis, although with stronger signal in the nervous system. This seems to constitute an exception, since in most metazoans GATA123 genes appear tightly linked to ectoderm-derived (including non-neural ectoderm) tissue development (Gillis et al., 2007; Lentjes et al., 2016; Nardelli et al., 1999; Read et al., 1998; Tsarovina et al., 2004). In *Botryllus*, the two genes exhibited distinct, non-overlapping expression patterns during palleal bud development. *GATAb* was detected in the arising inner vesicle of the budlet at stage A1 and A2 (Fig. 2A). In B1 and B2 stages, the budlet expression of *GATAb* was not detected (not shown), but reappeared at the stage C1, where a few cells weakly express *GATAb* transcripts in the forming peribranchial chambers (Fig. 2B). In budlets at stage C2 and D, the signal detected was more intense, and the area of expression of *GATAb* was expanded, covering the external side of both left and right peribranchial chamber epithelia (Fig. 2C, D). In these tissues, the pattern of expression remained globally constant until the primary bud forms at stage A1 and A2. Compared to budlets at stage C2 and D, detection of *GATAb* in the primary buds at stage A1-A2 was slightly weaker (Fig. S6A), however this could be due to probe penetration. When the primary buds reach stage B1, the peribranchial epithelia stops expressing *GATAb*. This interval coincides with the interruption of signal detection in the budlet at stage B1 and B2 (see Table 1). In addition *GATAb* expression was also found from budlet at stage D to primary bud at stage A2 in the branchial chamber epithelium (Fig. 2D, arrowhead), and later in stage B1, in the epithelium of the forming intestine (Fig. S6B).

Otx expression was detected in the budlet starting from stage B1 and B2 (Fig. 2E). *Otx* positive cells are located anteriorly, on the dorsal side of the budlet inner vesicle.

While the budlet grows, the signal remained restricted to the dorsal side and expanded to both left and right side of the inner epithelium (Fig. 2F). As organogenesis progresses from C1 to

stage D, *Otx* transcripts could be detected in the dorsal tube, and, in defined areas of the branchial and peribranchial epithelia surrounding the dorsal tube (Fig. 2G). This dorso-anterior pattern was maintained in the budlet at stage D, where, within the tube, only the anterior-most cells expressed the transcripts (Fig. 2H). Similar patterns were observed in the primary buds at stage A1 and A2. In primary buds from stage B1 to C2, *Otx* is detected in the cells at the anterior basis of the neural gland and around the oral siphon (Fig. S6C, D).

Pattern of expression of endoderm-associated TFs during PB

To assess formation of endodermal tissues during PB, we followed the expression of *Fox-A*1, *Fox-A*2 and *GATA4/5/6* (*GATAa* in ascidians) orthologs. Both Fox genes are associated with gut formation and definitive endodermal tissues in metazoans (Friedman and Kaestner, 2006), while GATA4/5/6 genes, in addition to endoderm formation, are also expressed in cardiac progenitors (Patient and McGhee, 2002).

In the budlets at stage B2, *Fox-A*1 showed a weak signal confined in two domains on the anterior and posterior sides of the bud inner vesicle (Fig. 3A). At stage C1, the posterior expression expanded into the gut rudiment. Another domain of expression was detected dorsally in the epithelium of the inner vesicle of the budlet. This domain covered both posterior and anterior extremities (see Fig. 3B) of the dorsal side of the inner vesicle epithelium, but not its central area, where the dorsal tube sprouts. In budlet C2, *Fox-A*1 expression was detected in the gut rudiment, however, from next stage D to later primary bud stages, the signal progressively disappeared from most of the gut rudiment except in its most posterior end, where the oesophagus develops (Fig. 3C, D; Fig. S7A). In this latter region *Fox-A*1 expression was strongly detected until the adult.

In addition, other tissues of the primary buds showed consistent *Fox-A*1 expression. These comprised epithelial cells forming the endostyle rudiment along the A/P axis from stage A1 to

C2 (Fig. S7B). Cells expressing *Fox-A*1 were found in forming stigmata; *Fox-A*1 was only detected in cells at both A/P extremities of the newly perforated stigma (Fig. S7A), and in primary buds B1 to C2, in the posterior extremity of the dorsal tube (Fig. S9C, D). *Fox-A*2, was detected in the gut rudiment of the budlets. In primary buds, it was expressed exclusively in tissues associated with the digestive system (data not shown).

The expression of *GATAa* was firstly detected in the budlet at stage B1 in a group of cells covering almost all the posterior half of the inner vesicle (Fig. 3E). At stage B2 the region expressing *GATAa* is confined to a patch of about 10 to 15 cells positioned ventrally in the posterior half of the budlet (Fig. 3F). During the transition from stage B2 and stage C1/C2, the posterior side of the budlet evaginates, forming the borders of the future gut rudiment. In this area, that progressively elongates forming the digestive tract (Manni et al., 2014), *GATAa* signal was detected (Fig. 3G, H). In the primary bud at stage A1 to B2, gut regionalization is morphologically observable. *GATAa* expression was found to be restricted to the stomach rudiment, and absent from intestine and associated glands. The signal observed in the stomach decreased progressively as the blastogenetic cycle progresses and eventually disappears at the transition to adult. *GATAa* transcripts were also transiently detected, in clusters of cells located ventrally, on the right side of the primary bud (A1), where the organogenesis of the heart occurs (Fig. S7D). Finally, *GATAa* transcripts could also be detected in follicle cells surrounding mature oocytes in sexually mature colonies (Fig. S7C).

Pattern of expression of mesoderm-associated TFs during PB

To investigate the deployment of mesoderm related genes during palleal budding, we chose to follow the expression of genes coding the homeodomain protein *Gsc*, and the T-box proteins *Bra* and *Tbx2/3* (Brunet et al., 2013; José-Edwards et al., 2013; Niehrs et al., 1994; Ribeiro et al., 2007). *Gsc* transcript were first detected in the budlets at stage B1 and B2 where the

whole inner vesicle was labelled (Fig. 4A). Similar expression was observed in the budlet at early stage C1 in almost the whole inner vesicle except for the posterior evaginating epithelium that will form the gut rudiment (Fig. 4B). In C1, the signal was still detectable in the branchial and peribranchial chambers epithelia. In the budlet at C2 stage, the signal could no longer be detected from the ventral side of the budlet and was restricted to the rudiment of the branchial chamber epithelium, specifically on the dorsal side (Fig. 4C), the latter domain of expression is maintained in later stages, from budlet at stage D (see Fig. 4D) to the primary bud at stage B2, with notably stronger expression around the oral siphon. Although most of the dorsal cells exhibit *Gsc* expression, it is not the case for the structures involved in the formation of the central nervous system (CNS) such as in the dorsal tube and in the cerebral ganglion (Fig. S8A, B).

In early budlet (A2) *Tbx2/3* was detected weakly in a few cells located posteriorly to the arching budlet in the inner epithelia (data not shown). In budlets B1-B2, the signal was relatively stronger. At stage B2, *Tbx2/3* positive cells were detected in two distinct domains at posterior-dorsal and anterior-ventral ends of the inner vesicle (Fig. 4E). At the onset of stage C, a very distinct domain was found in the invaginating epithelium of the inner vesicle, located centrally in the budlet where the branchial cavity will separate from the peribranchial chambers (Fig. 4F). At the same stage C, a group of cells located dorsally in the inner vesicle also expressed *Tbx2/3* transcripts (Fig. 4F), in the area where the CNS is forming. While the budlet compartmentalization progresses from C1 to C2, the signal is restricted to the anterior-dorsal cells of the peribranchial chambers epithelia (Fig. 4G). In the budlet at stage D, *Tbx2/3* expression strongly decreased in the peribranchial epithelia, while cells at the posterior extremity of the dorsal tube exhibited distinct signal (Fig. 4H). *Tbx2/3* expression could be detected in dorsal tube cells in the primary buds until stage C2. These cells are located at both the anterior and the posterior extremities of the dorsal tube, but not in its median region (Fig.

S8C). *Tbx2/3* was also observed in scattered cells located between the dorsal tube and the oral siphon rudiment and in the mesenchyme in the primary bud at stage A1 (Fig. S8C). From primary bud at stage A2 to stage D, *Tbx2/3* was detected in the latter dorsal domain but also in ventral domains such as the forming stomach and in pair crests formed by the branchial epithelia, flanking the endostyle rudiment along the A/P axis (Fig. S8D).

Transcripts of the TF *Bra* could only be only detected in primary buds from stage B1 to stage C2. *Bra* expression was observed in localized area at the posterior end of the dorsal tube (Fig. S9A, B). The expression domain overlaps temporally but also spatially with the *Tbx2/3* and *Fox-A*1 domains in primary bud dorsal tube (Fig. S8C and S9C, D).

Vascular bud morphology and staging

Due to the lack of anatomical details on *B.schlosseri* VB, and in order to assess whether, as in PB, stereotyped morphogenetic stages could be identified during the early steps of regeneration, we described the initial phases of vascular bud formation. More than 75% of the first observable vascular buds (n=41) were detected between 2 and 5 days following surgery: The first regenerative structure observable by tubulin labelling is a cluster of approximately 15 microns of diameter (Stage 1, Fig. 5D), located in the vascular lumen. The clusters developed into a hollow vesicle and often exhibited polarized morphology (Stage 2 and 3, Fig. 5E).This polarity was rapidly lost while the bud grew in size (≈ 40 µm), reaching a spherical shape (≈60µm), comparable to the B2 stage of palleal budlets (Stage 4, Fig. 5F). Following these early stereotyped stages, vascular buds, underwent epithelial folds and subsequent organogenesis (Stage 5, Fig. 5G). From this stage on, the variability in morphologies and growth rates prevents the identification of organs and body axes (Fig. S10).

Pattern of expression of germ layers-associated TFs during VB

In order to assess the presence and the domains of expression of germ layers related TFs during VB we followed by FISH the expression of *GATAb*, *Otx*, *Fox-A1*, *GATAa*, *Gsc*, *Tbx2/3* and *Brachyury* on buds collected at early stages (from stage 2 to stage 5). With the exception of *Bra*, the candidate genes studied during PB were all found expressed during VB. Due to their extremely small sizes, and the difficulty to detect them, vascular buds at stage 1 were rarely observed and TF expression at such stages was not considered.

In early regenerative steps (from stage 1 to stage 4) *GATAb* was not found expressed in the vascular buds (Fig. 6A), while *Otx*, the other ectoderm-related marker, was found expressed faintly in few cells of the bud, but never widespread over the inner vesicle (Fig. 6B) Conversely, vascular buds at stage 5 clearly express both *GATAb* and *Otx*. *GATAb* transcripts in the epithelia lining the vascular endothelium were detected on epithelia flanking the sides of the vascular bud (Fig. 6G). Considering the position of the labelled tissues relative to the gut rudiment and their morphology, we inferred these were the peribranchial epithelia of the vascular bud. At the same stage, *Otx* was also expressed at the most anterior position of the putative peribranchial epithelia (Fig. 6H). *Fox-A1* was detected in early vascular buds at stage 3 (Fig. 6C), while at stage 5, the folding inner epithelia show patchy staining (Fig. 6I). *GATAa* was also seen expressed from stages 3. The expression is restricted in a patch of labelled cells in stage 3 (Fig. 6 D). In stage 5, *GATAa* expression could still be observed in a small area of the vascular bud, although not allowing organ identification (Fig. 6J).

At stage 2 of VB, *Gsc* showed relatively strong expression in a patch of cells in the inner vesicle (Fig. 6E). In later vascular buds, *Gsc* showed expression as well, although in smaller areas than in palleal buds (Fig. 6K). In early buds (stages 3 and stage 4) *Tbx2/3* is expressed in the inner vesicles in two, diametrically opposed domains (Fig.6F). In late buds, we observed a relatively widespread signal inside the inner vesicle (Fig. 6L). However, due to the

lack of morphological references it was not possible to identify anatomical structures with certainty.

Distruption of *GATAa* expression arrest palleal bud development

As a mean to validate the FISH results and as a first step to address TF function during PB, we used siRNA technique to target *GATAa* mRNA. *Botryllus* colonies were injected at stage A1 or D with siRNA for *GATAa* which was shown to be effective by the lack of FISH signal in specimens fixed 5 days after treatment (Fig.7). Treated colonies started exhibiting a distinct phenotype compared to PBS-injected and GFP-siRNA injected colonies after two or three days of treatment. Adult and bud bodies contracted towards the centre of the colony, leaving an empty space between the anterior tip of the adult and the surrounding peripheral vasculature (Fig.7C, C', D and D'). No particular defect could be detected in individual zooids at this stage. The primary buds were smaller in size than in the control animal, although they displayed normal morphology and physiological behaviour, i.e. regular heart beating and muscular function (contractions and feeding, data not shown). The budlets interrupted development at the B1/B2 stage, when they start forming a closed double vesicle (Fig. 7A, A'). The palleal bud development of control colonies progressed normally (Fig. 7A' D'). Histological observations confirmed live observations (data not shown). In colonies treated starting from stage B2 we observed the lack of gut evagination in the primary buds and the absence of budlet development (Fig. 7B, B'). Seven to eight days after treatment, the colonies do not restart the normal palleal bud development and eventually die.

Discussion

We characterized the expression patterns of selected transcription factors through the developmental stages of PB and during the early steps of the regenerative VB. It is not yet technically possible to track cell lineages *in vivo* during these processes, but for the first time

we were able to follow the fate of a differentiating tissue during asexual development and partially during a regenerative process. The continuous expression of developmental TFs allowed us to deduce the adult derivatives of several cell lineages and track them back to their early cellular precursors in the palleal budlet.

Redeployment of developmental TFs in PB and VB

Six of the seven selected TFs, showed expression during the early phase of PB and VB. The exception was *Brachyury*, which was only expressed in the primary bud during PB, and not detected during VB. There was a clear correspondence between the expression of each TF in structures and organs developed asexually with their known expression profiles and the tissue determination during embryogenesis in ascidians, and in other chordates such as zebrafish, mouse, xenopus and cephalochordates. For instance, *Botryllus GATAa* and *Fox-A1* were detected mostly in organs of endodermal origin, such as the digestive tract and in the endostyle. This mirrors expression in embryos of solitary ascidians (Di Gregorio et al., 2001; Olsen et al., 1999) and other bilaterians (Arceci et al., 1993; Capo-Chichi et al., 2005; De-Leon, 2011; Friedman and Kaestner, 2006; Lee et al., 2005). Similarly, the highly conserved role of GATA4/5/6 genes in chordate heart patterning (Kikuchi et al., 2010; Ragkousi et al., 2011) could well be co-opted in PB, as suggested by the transient expression of *GATAa* in putative cardiomyocytes (Fig. S7D), before the heart acquires its final tubular shape (Berrill, 1941).

TFs associated with ectodermal fates also showed expression patterns during PB reminiscent of embryogenesis in other chordates. For *Otx*, the expression profile was characterized by an antero-dorsal localisation in the budlets and primary buds, and expression in neural precursors and in non-neural surrounding tissues. These characteristics resemble the expression of OTX in other chordates's embryogenesis, where it is required in neural plate precursor cells and in

surrounding endoderm to promote cell migration and further differentiation of neural progenitors (Hudson and Lemaire, 2001; Klein and Li, 1999; Rhinn et al., 1998; Simeone, 1998; Wada et al., 1996; Williams and Holland, 1998). *GATAb* is also expressed in the peribranchial epithelia. The embryonic origin of this tissue in ascidians is still controversial, as some authors consider it of ectodermal origin (Scott, 1934, 1946; Manni et al., 2002), while others suggest an endodermal origin (Hirano and Nishida, 2000). Hypotheses of both origins of the ascidian peribranchial epithelium might be correct as they were assessed from studies in different ascidians orders: Enterogona and Pleurogona respectively (Kawamura et al., 2008). GATA1/2/3 genes (the orthologs of *GATAb*) expression in vertebrates and non-vertebrates is tightly associated with the formation of ectodermal tissues (Gillis et al., 2007; Read et al., 1998; Tsarovina et al., 2004). Our results concerning the expression of *GATAb* thus support the hypothesis of an ectodermal identity for the peribranchial epithelia in *B.schlosseri*, at least in the palleal bud, regardless to their embryonic origin. In addition, a peak of *GATAb* expression was observed precisely in the region where new budlets will originate (Fig. 2D) indicating a possible role in the initiation of the budding process itself. Hence, these results argue against an endodermal origin of peribranchial epithelium in Pleurogona (Hirano and Nishida, 2000) and of a higher regenerative/budding capacity in endodermal versus ectodermal tissues in colonial ascidians (Brown and Swalla, 2012; Kawamura et al., 2008).

It is not so straightforward to correlate TF expression to development of mesoderm- derived tissues. For example, *Tbx2/3*, is not an exclusive mesoderm marker, and is expressed in multiple domains in *Botryllus* (Fig. S8C,D), as well as in *Ciona* larva, where it is expressed in notochord, CNS and epidermis (José-Edwards et al., 2013). *Gsc* expression and function are very poorly documented in ascidians, where it has been reported to be expressed ubiquitously in early stages, from the fertilized egg to the neurula, while later and until late tailbud stage,

cells expressing *Gsc* are found in the neck and head (Imai et al., 2004). In the budlet, we observed ubiquitous expression of *Gsc* in the double vesicle, which became restricted to the dorsal epithelia in stages C1/C2. The same region also expresses *Tbx2/3*. These dorsal expression patterns, in particular for *Gsc*, are reminiscent of expression of orthologous genes in the dorsal endomesoderm of vertebrate embryos (Blum et al., 1992; Middleton et al., 2009; Niehrs et al., 1994), suggesting a potential role of the budlet dorsal epithelia in re-setting mesodermal lineages during PB.

Analysis of the "mesoderm-specific" TF *Brachyury* revealed unexpectedly a possible change in role to neurogenesis. In *Botryllus* we only detected expression late during PB, in primary buds B2 and C2, and only in the posterior most cells of the dorsal tube, a structure that has been associated with neurogenesis (Burighel et al., 1998; Manni et al., 2001; Manni et al., 2014). While in vertebrates *Brachyury* is widely expressed in mesodermal tissues, In *Ciona* and other solitary ascidian embryos, *Brachyury* expression is restricted to the notochord. Recent work has shown that *Ci-Bra* has numerous direct target genes in the notochord, including *Ci-Tbx2/3* (Katikala et al., 2013). *Ci-Tbx2/3* mediates *Ci-Bra* function by regulating a high number of downstream targets thought, notably, to promote notochord cells convergent extension (José-Edwards et al., 2013). In *Botryllus*, we found *Tbx2/3* co-expressed in the same neural structure as *Brachyury*, but it was detected significantly earlier (primary bud A1 versus primary bud B2). In addition, *Fox-A1* was also localized with *Bra* in the posterior most cells of the dorsal tube at the same stages. In *Ciona* embryos, promoters of *Bra* and *Fox-Aa* (the homolog of FOX-A2) have been shown to be sufficient to drive gene expression in the notochord (Passamaneck et al., 2009). Unfortunately, the low expression of such TFs does not allow to perform double FISH, as it has successfully done for other highly expressed genes (Langenbacher et al., 2015). The presence of several components of the mesoderm GRN in the dorsal tube may suggest that the nature of this structure is not only neurogenic, and the

cells delaminating from the dorsal tube (Manni et al., 1999) could possibly contribute to other cell fates (Ricci et al. *in preparation*). Conversely, a module of the mesoderm GRN could be co-opted and/or wired differently in order to drive a neural fate.

The different intrinsic nature of the sexual, asexual, and regenerative developmental processes, makes their comparison a challenging task. For instance, embryogenesis leads to an adult zooid, but includes both a tadpole stage and metamorphosis, while in PB and VB the source of the new zooids are different adult cells. Given these heterochronies and different ontologies, it is not surprising that expression patterns cannot always be correlated and can explain some important differences in gene expression, such as the patterns of *Bra* and *Tbx2/3*, or the patterns of expression, which do not suggest a function in early ectoderm specification of *GATAa* or *Fox-A*, as observed in *Ciona intestinalis* (Lamy et al., 2006; Rothbächer et al., 2007).

In this context it is worth noting that we tested expression of multiple developmental regulatory genes that we could not detect neither by FISH nor by PCR during PB and during VB. In particular *ZicL*, *Ephrin* and *Nodal* could not be detected neither by FISH nor by PCR (Fig. S11). On the other hand, *Twist* was detected by PCR at all palleal bud stages but not by FISH despites several probes have been used. Such key TFs are however essential in mesendoderm formation, myogenesis, and induction of neural fate during embryogenesis (Anno et al., 2006; Imai et al., 2009; Mita and Fujiwara, 2007; Noda, 2011; Stolfi et al., 2011; Tokuoka et al., 2005; Wada and Saiga, 1999). Their absence during non-embryonic developments may suggest that part of the mesendodermal GRNs is bypassed, and/or that different modules are in place, it could also suggests the presence of isoforms specifically expressed during PB.

Tissue fate regionalization in adult epithelia

In *B. schlosseri* and other colonial ascidians, both PB and VB seem to share a common ontogenetic stage: a triplobastic vesicle formed by two mono-layered polarized epithelia that sandwich a mesenchyme of circulating haemoblasts (corresponding to stage B2 of *Botryllus* palleal bud, or stage 3 in VB) (Fig 1C, Fig 2F, H, Nakauchi, 1982; Tiozzo et al., 2008a). Merely based on visual morphological characteristics, this presumptive phylotypic stage of asexual development has been previously compared to a blastula (Rinkevich et al., 1995; Voskoboynik et al., 2007). Data presented here (Fig. 2I, 3I, 4I), show that the double vesicle exhibits regionalization, notably for ecto- (neural, *Otx*) and endodermal identities (guts, *GATAa*). This supports the idea that early spatial segregation of cell fate domains in the double vesicle resembles those in a blastula and is consistent with this being a phylotipic stage for budding. Nevertheless, directly comparing any stage of asexual development to an embryonic structure, should be viewed with extreme caution: unlike the ascidian embryo, fate specification in buds does not involve inheritance of localised determinants from the egg, rather the buds grow by rapid scattered proliferative activity, with no defined cell division pattern (data not shown). This is dramatically different from the stereotypical cleavage pattern of ascidian embryogenesis, which segregates maternal determinants and defines cell fates through successive cleavage divisions without growth (Hudson et al., 2013). The variation in the patterning of the palleal and vascular buds suggests that their development involved extensive intracellular signalling and is probably regulative in nature. Complementary experiments such as bud bisection, or bud tissue transplant would be interesting to test this hypothesis (Lawrence and Levine, 2006; Munro and Odell, 2002; Sabbadin et al., 1975).

A further obstacle on comparing embryonic and non-embryonic developments is represented by the uncertain nature of bud origin, which in colonial ascidians is still not fully characterized (Kürn et al., 2011; Stolfi and Brown, 2015). Whereas the anatomical origin of the epidermal tissues of palleal and vascular buds is easily recognizable, i.e. the primary bud

epidermis and the vessels endothelium respectively (Manni et al., 2014; Sabbadin et al., 1975; see Fig. 1 and 5), the cellular origin of budlet and vascular bud inner vesicle is not clear. Even in the stereotyped PB, the participation of mesenchymal cells, in addition to the peribranchial epithelium, cannot be ruled out. Indeed, knowing the nature of the buds will help to better understand the later regionalization of tissue fates. Loss-of-function of *GATAa* confirmed that preventing the correct development of one of these regions blocks further tissue specification, blocking formation of the digestive tract (Fig. 7B'), or leading to the arrest of the bud morphogenesis, depending on the timing of siRNA knockdown (Fig. 7A, B, D'). It is not clear if *GATAa* is required for the morphogenetic event only, i.e., the gut evagination in budlet stage C, and/or for commitment into an endodermal-like lineage. On the other hand, it is not possible to rule out the contribution of pluripotent haemoblasts to specific domain of the inner vesicle. The specification of such cells could indeed occur upstream the determination observed in the described domains. Further functional analyses of upstream TFs will be then crucial. Finally, even considering the similarity between *Botryllus* embryogenesis with the one of the closely related species *Halocynthia rorezi* (Brown and Swalla, 2012; Hirano and Nishida, 2000; Kumano et al., 2006; Kumano et al., 2014; Ogasawara et al., 2006; Tanaka et al., 1996; Wada et al., 1996; Wada et al., 2004; supp.video V1, V2), and despite the robustness of embryonic development among ascidians, including colonial species (Bertrand et al., 2003; Brown and Swalla, 2012; Hotta et al., 2000; Hudson and Lemaire, 2001; José-Edwards et al., 2013; Lamy et al., 2006; Lemaire, 2009; Stolfi and Brown, 2015; Wada et al., 2004) we cannot rule out the possibility that *Botryllus* embryogenesis follows completely different developmental trajectories.

One program for two developments?

The partial redeployment of developmental programs during asexual development, and particularly regeneration, is not a novel idea in the literature (Kürn et al., 2011; Vorontsova

and Liostner, 1960). Nonetheless, only a few studies have compared gene expression during the two processes (Bely and Wray, 2001; Burton and Finnerty, 2009; Martinez et al., 2005).

PB and VB have distinct cellular origins: peribranchial epithelia versus circulating haemoblasts/vascular endothelia, and distinct physiological cues: asexual growth versus injury-triggered regeneration. However, the spatio-temporal expression of key embryonic TFs during asexual development suggests that a common "bud fate map" applies for both vascular and palleal bud development, as they exhibit comparable expression profiles, notably at the double vesicle stage (summarized in Fig. 8 and Fig. 6A-F). Furthermore, our results strongly indicate that the early stages of PB and VB likely share a common developmental program, different from embryogenesis. Of course, this is not surprising, as asexual developments occur in a vastly different physical environment than embryogenesis. For example, it would be difficult to set up morphogen gradients in an environment of rapid blood flow that occurs during PB and VB, thus certain specification pathways cannot be re-used in asexual development. This is reflected in unique phenotypes that occur during VB, such as axis duplication, *situs inversus* or organs defects, which have not been observed in embryogenesis and are likely a consequence of the differences in the physical environment (Sabbadin et al., 1975; Voskoboynik et al., 2007.).

The ability of colonial ascidians to initiate what seems to be the same developmental process in different biological contexts and from different cell populations is highly intriguing. Addressing those questions, in particular elucidating the signal(s) that induce different kind of budding can provide great insights on the evolution of chordate regenerative abilities, but also on the plasticity of developmental programs.

Acknowledgements

We would like to thanks M. Khamla for his contribution with the artwork. We also thank Dr. P. Lapébie and W.Q. Gillis for providing us trimmed and aligned amino-acid sequences of metazoan Fox, Tbx and GATA gene families. We thank Prof. Anthony De Tomaso and Dr. Evelyn Houliston for their comments and suggestions. This work was supported by AFMTelethon grand (#16611), IRG Marie Curie grant (#276974), ANR (ANR-14-CE02-0019-01) and IDEX Super (INDIBIO). L.R. was supported by an UPMC-EMERGENCE grant and by an FRM grant (#FDT20140931163).

References

Anno, C., Satou, A. and Fujiwara, S. (2006). Transcriptional regulation of ZicL in the Ciona intestinalis embryo. *Dev. Genes Evol.* **216**, 597–605.

Arceci, R. J., King, a a, Simon, M. C., Orkin, S. H. and Wilson, D. B. (1993). Mouse GATA-4: a retinoic acid-inducible GATA-binding transcription factor expressed in endodermally derived tissues and heart. *Mol. Cell. Biol.* **13**, 2235–2246.

Beby, F. and Lamonerie, T. (2013). The homeobox gene Otx2 in development and disease. *Exp. Eye Res.* **111**, 9–16.

Bely, a E. and Wray, G. a (2001). Evolution of regeneration and fission in annelids: insights from engrailed- and orthodenticle-class gene expression. *Development* **128**, 2781–2791.

Berrill, N. J. (1941). The Development of the Bud in Botryllus. *Biol Bull* **80**, 169–184.

Berrill, N. J. (1948). Budding and the reproductive cycle of Distaplia. *Q. J. Microsc. Sci.* **89**,

253–89.

Berrill, N. J. (1951). Regeneration and Budding in Tunicates. *Biol. Rev.* **26**, 456–475.

Bertrand, V., Hudson, C., Caillol, D., Popovici, C. and Lemaire, P. (2003). Neural Tissue in Ascidian Embryos Is Induced by FGF9/16/20, Acting via a Combination of Maternal GATA and Ets Transcription Factors. *Cell* **115**, 615–627.

Blum, M., Gaunt, S. J., Cho, K. W., Steinbeisser, H., Blumberg, B., Bittner, D. and De Robertis, E. M. (1992). Gastrulation in the mouse: the role of the homeobox gene goosecoid. *Cell* **69**, 1097–1106.

Boyle, M. J. and Seaver, E. C. (2010). Expression of FoxA and GATA transcription factors correlates with regionalized gut development in two lophotrochozoan marine worms: Chaetopterus (Annelida) and Themiste lageniformis (Sipuncula). *Evodevo* **1**, 2.

Brown, F. D. and Swalla, B. J. (2012). Evolution and development of budding by stem cells: ascidian coloniality as a case study. *Dev. Biol.* **369**, 151–62.

Brown, F. D., Keeling, E. L., Le, A. D. and Swalla, B. J. (2009). Whole body regeneration in a colonial ascidian, Botrylloides violaceus. *J. Exp. Zool. B. Mol. Dev. Evol.* **312**, 885–900.

Brown, L. E., King, J. R. and Loose, M. (2014). Two different network topologies yield bistability in models of mesoderm and anterior mesendoderm specification in amphibians. *J. Theor. Biol.* **353**, 67–77.

Brunet, T., Bouclet, A., Ahmadi, P., Mitrossilis, D., Driquez, B., Brunet, A.-C., Henry, L., Serman, F., Béalle, G., Ménager, C., et al. (2013). Evolutionary conservation of early mesoderm specification by mechanotransduction in Bilateria. *Nat. Commun.* **4**, 2821.

Burighel, P., Lane, N. J., Zaniolo, G. and Manni, L. (1998). Neurogenic role of the neural gland in the development of the ascidian, Botryllus schlosseri (Tunicata, Urochordata). *J. Comp. Neurol.* **394**, 230–41.

Burton, P. M. and Finnerty, J. R. (2009). Conserved and novel gene expression between regeneration and asexual fission in Nematostella vectensis. *Dev. Genes Evol.* **219**, 79–87.

Capella-Gutiérrez, S., Silla-Martínez, J. M. and Gabaldón, T. (2009). trimAl: A tool for automated alignment trimming in large-scale phylogenetic analyses. *Bioinformatics* **25**, 1972–1973.

Capo-Chichi, C. D., Rula, M. E., Smedberg, J. L., Vanderveer, L., Parmacek, M. S., Morrisey, E. E., Godwin, A. K. and Xu, X. X. (2005). Perception of differentiation cues by GATA factors in primitive endoderm lineage determination of mouse embryonic stem cells. *Dev. Biol.* **286**, 574–586.

De-Leon, S. B. T. (2011). The conserved role and divergent regulation of foxa, a pan-eumetazoan developmental regulatory gene. *Dev. Biol.* **357**, 21–26.

Delsuc, F., Brinkmann, H., Chourrout, D. and Philippe, H. (2006). Tunicates and not cephalochordates are the closest living relatives of vertebrates. *Nature* **439**, 965–8.

Di Gregorio, a, Corbo, J. C. and Levine, M. (2001). The regulation of forkhead/HNF-3beta expression in the Ciona embryo. *Dev. Biol.* **229**, 31–43.

Doglio, L., Goode, D. K., Pelleri, M. C., Pauls, S., Frabetti, F., Shimeld, S. M., Vavouri, T. and Elgar, G. (2013). Parallel Evolution of Chordate Cis-Regulatory Code for Development. *PLoS Genet.* **9**, 1–16.

Drummond, A. J., Suchard, M. a., Xie, D. and Rambaut, A. (2012). Bayesian phylogenetics with BEAUti and the BEAST 1.7. *Mol. Biol. Evol.* **29**, 1969–1973.

Dumollard, R., Hebras, C., Besnardeau, L. and McDougall, A. (2013). Beta-catenin patterns the cell cycle during maternal-to-zygotic transition in urochordate embryos. *Dev. Biol.* **384**, 331–342.

Erwin, D. H. (2009). Early origin of the bilaterian developmental toolkit. *Philos. Trans. R. Soc. Lond. B. Biol. Sci.* **364**, 2253–2261.

Friedman, J. R. and Kaestner, K. H. (2006). The Foxa family of transcription factors in development and metabolism. *Cell. Mol. Life Sci.* **63**, 2317–2328.

Gasparini, F., Manni, L., Cima, F., Zaniolo, G., Burighel, P., Caicci, F., Franchi, N., Schiavon, F., Rigon, F., Campagna, D., et al. (2015). Sexual and asexual reproduction in the colonial ascidian Botryllus schlosseri. *Genesis* **53**, 105–120.

Gillis, W. J., Bowerman, B. and Schneider, S. Q. (2007). Ectoderm- and endomesoderm-specific GATA transcription factors in the marine annelid Platynereis dumerilli. *Evol. Dev.* **9**, 39–50.

Gillis, W. Q., Bowerman, B. a and Schneider, S. Q. (2008). The evolution of protostome GATA factors: molecular phylogenetics, synteny, and intron/exon structure reveal orthologous relationships. *BMC Evol. Biol.* **8**, 112.

Haupaix, N., Stolfi, A., Sirour, C., Picco, V., Levine, M., Christiaen, L. and Yasuo, H. (2013). p120RasGAP mediates ephrin/Eph-dependent attenuation of FGF/ERK signals during cell fate specification in ascidian embryos. *Development* **140**, 4347–52.

Hinman, V. F., Becker, E. and Degnan, B. M. (2000). Neuroectodermal and endodermal expression of the ascidian Cdx gene is separated by metamorphosis. *Dev. Genes Evol.* **210**, 212–6.

Hirano, T. and Nishida, H. (2000). Developmental fates of larval tissues after

metamorphosis in the ascidian, Halocynthia roretzi. II. Origin of endodermal tissues of the juvenile. *Dev. Genes Evol.* **210**, 55–63.

Horikawa, Y., Matsumoto, H., Yamaguchi, F., Ishida, S. and Fujiwara, S. (2013). Transcriptional regulation in the early ectodermal lineage of ascidian embryos. *Dev. Growth Differ.* **55**, 776–785.

Hotta, K., Takahashi, H., Asakura, T., Saitoh, B., Takatori, N., Satou, Y. and Satoh, N. (2000). Characterization of Brachyury-downstream notochord genes in the Ciona intestinalis embryo. *Dev. Biol.* **224**, 69–80.

Hudson, C. and Lemaire, P. (2001). Induction of anterior neural fates in the ascidian Ciona intestinalis. *Mech. Dev.* **100**, 189–203.

Hudson, C., Kawai, N., Negishi, T. and Yasuo, H. (2013). B-Catenin-Driven Binary Fate Specification Segregates Germ Layers in Ascidian Embryos. *Curr. Biol.* **23**, 491–495.

Imai, K. S., Satoh, N. and Satou, Y. (2002). Region specific gene expressions in the central nervous system of the ascidian embryo. *Mech. Dev.* **119 Suppl** , S275–7.

Imai, K. S., Hino, K., Yagi, K., Satoh, N. and Satou, Y. (2004). Gene expression profiles of transcription factors and signaling molecules in the ascidian embryo: towards a comprehensive understanding of gene networks. *Development* **131**, 4047–58.

Imai, K. S., Stolfi, A., Levine, M. and Satou, Y. (2009). Gene regulatory networks underlying the compartmentalization of the Ciona central nervous system. *Development* **136**, 285–293.

Izzard, C. S. (1973). Development of polarity and bilateral asymmetry in the palleal bud of Botryllus schlosseri (Pallas). *J. Morphol.* **139**, 1–25.

José-Edwards, D. S., Oda-Ishii, I., Nibu, Y. and Di Gregorio, A. (2013). Tbx2/3 is an

essential mediator within the Brachyury gene network during Ciona notochord development. *Development* **140**, 2422–33.

Katikala, L., Aihara, H., Passamaneck, Y. J., Gazdoiu, S., José-Edwards, D. S., Kugler, J. E., Oda-Ishii, I., Imai, J. H., Nibu, Y. and Di Gregorio, A. (2013). Functional Brachyury Binding Sites Establish a Temporal Read-out of Gene Expression in the Ciona Notochord. *PLoS Biol.* **11**,.

Kawamura, K., Sugino, Y., Sunanaga, T. and Fujiwara, S. (2008). Multipotent epithelial cells in the process of regeneration and asexual reproduction in colonial tunicates. *Dev. Growth Differ.* **50**, 1–11.

Kikuchi, K., Holdway, J. E., Werdich, A. a, Anderson, R. M., Fang, Y., Egnaczyk, G. F., Evans, T., Macrae, C. a, Stainier, D. Y. R. and Poss, K. D. (2010). Primary contribution to zebrafish heart regeneration by gata4(+) cardiomyocytes. *Nature* **464**, 601–605.

Klein, W. H. and Li, X. (1999). Function and evolution of Otx proteins. *Biochem. Biophys. Res. Commun.* **258**, 229–233.

Kumano, G. and Nishida, H. (2007). Ascidian embryonic development: an emerging model system for the study of cell fate specification in chordates. *Dev. Dyn.* **236**, 1732–47.

Kumano, G., Yamaguchi, S. and Nishida, H. (2006). Overlapping expression of FoxA and Zic confers responsiveness to FGF signaling to specify notochord in ascidian embryos. *Dev. Biol.* **300**, 770–784.

Kumano, G., Negoro, N. and Nishida, H. (2014). Transcription factor Tbx6 plays a central role in fate determination between mesenchyme and muscle in embryos of the ascidian, Halocynthia roretzi. *Dev. Growth Differ.* **56**, 310–322.

Kürn, U., Rendulic, S., Tiozzo, S. and Lauzon, R. J. (2011). Asexual propagation and regeneration in colonial ascidians. *Biol. Bull.* **221**, 43–61.

Laird, D. J., Chang, W.-T., Weissman, I. L. and Lauzon, R. J. (2005). Identification of a novel gene involved in asexual organogenesis in the budding ascidian Botryllus schlosseri. *Dev. Dyn.* **234**, 997–1005.

Lamy, C., Rothbächer, U., Caillol, D. and Lemaire, P. (2006). Ci-FoxA-a is the earliest zygotic determinant of the ascidian anterior ectoderm and directly activates Ci-sFRP1/5. *Development* **133**, 2835–2844.

Langenbacher, A. D., Rodriguez, D., Di Maio, A. and De Tomaso, A. W. (2015). Whole-mount fluorescent in situ hybridization staining of the colonial tunicate Botryllus schlosseri. *Genesis* **53**, 194–201.

Lapébie, P., Ruggiero, A., Barreau, C., Chevalier, S., Chang, P., Dru, P., Houliston, E. and Momose, T. (2014). Differential Responses to Wnt and PCP Disruption Predict Expression and Developmental Function of Conserved and Novel Genes in a Cnidarian. *PLoS Genet.* **10**, e1004590.

Lauzon, R. J., Ishizuka, K. J. and Weissman, I. L. (2002). Cyclical Generation and Degeneration of Organs in a Colonial Urochordate Involves Crosstalk between Old and New: A Model for Development and Regeneration. *Dev. Biol.* **249**, 333–348.

Lawrence, P. a. and Levine, M. (2006). Mosaic and regulative development: two faces of one coin. *Curr. Biol.* **16**, 236–239.

Le Douarin, N. M. and Dupin, E. (2012). The neural crest in vertebrate evolution. *Curr. Opin. Genet. Dev.* **22**, 381–389.

Lee, C. S., Friedman, J. R., Fulmer, J. T. and Kaestner, K. H. (2005). The initiation of

liver development is dependent on Foxa transcription factors. *Nature* **435**, 944–947.

Lemaire, P. (2009). Unfolding a chordate developmental program, one cell at a time: Invariant cell lineages, short-range inductions and evolutionary plasticity in ascidians. *Dev. Biol.* **332**, 48–60.

Lemaire, P. (2011). Evolutionary crossroads in developmental biology: the tunicates. *Development* **138**, 2143–52.

Lemaire, P. and Gurdon, J. B. (1994). A role for cytoplasmic determinants in mesoderm patterning: cell-autonomous activation of the goosecoid and Xwnt-8 genes along the dorsoventral axis of early Xenopus embryos. *Development* **120**, 1191–1199.

Lemaire, P., Smith, W. C. and Nishida, H. (2008). Ascidians and the plasticity of the chordate developmental program. *Curr. Biol.* **18**, R620–31.

Lentjes, M. H., Niessen, H. E., Akiyama, Y., de Bruïne, A. P., Melotte, V. and van Engeland, M. (2016). The emerging role of GATA transcription factors in development and disease. *Expert Rev. Mol. Med.* **18**, e3.

Manni, L., Zaniolo, G. and Burighel, P. (1993). Egg Envelope Cytodifferentiation in the Colonial Ascidian Botryllus schlosseri (Tunicata). *Acta Zool.* **74**, 103–113.

Manni, L., Zaniolo, G. and Burighel, P. (1994). An unusual membrane system in the oocyte of the ascidian Botryllus schlosseri. *Tissue Cell* **26**, 403–412.

Manni, L., Lane, N. J., Sorrentino, M., Zaniolo, G. and Burighel, P. (1999). Mechanism of neurogenesis during the embryonic development of a tunicate. *J. Comp. Neurol.* **412**, 527–41.

Manni, L., Lane, N. J., Burighel, P. and Zaniolo, G. (2001). Are neural crest and placodes exclusive to vertebrates? *Evol. Dev.* **3**, 297–8.

Manni, L., Lane, N. J., Zaniolo, G. and Burighel, P. (2002). Cell reorganisation during epithelial fusion and perforation: the case of ascidian branchial fissures. *Dev. Dyn.* **224**, 303–13.

Manni, L., Zaniolo, G., Cima, F., Burighel, P. and Ballarin, L. (2007). Botryllus schlosseri: a model ascidian for the study of asexual reproduction. *Dev. Dyn.* **236**, 335–52.

Manni, L., Gasparini, F., Hotta, K., Ishizuka, K. J., Ricci, L., Tiozzo, S., Voskoboynik, A. and Dauga, D. (2014). Ontology for the Asexual Development and Anatomy of the Colonial Chordate Botryllus schlosseri. *PLoS One* **9**, e96434.

Martindale, M. Q., Pang, K. and Finnerty, J. R. (2004). Investigating the origins of triploblasty: "mesodermal" gene expression in a diploblastic animal, the sea anemone Nematostella vectensis (phylum, Cnidaria; class, Anthozoa). *Development* **131**, 2463–74.

Martinez, V. G., Menger, G. J. and Zoran, M. J. (2005). Regeneration and asexual reproduction share common molecular changes: upregulation of a neural glycoepitope during morphallaxis in Lumbriculus. *Mech. Dev.* **122**, 721–32.

Middleton, a. M., King, J. R. and Loose, M. (2009). Bistability in a model of mesoderm and anterior mesendoderm specification in Xenopus laevis. *J. Theor. Biol.* **260**, 41–55.

Milkman, R. (1967). Genetic and developmental studies on Botryllus schlosseri. *Biol. Bull.* **132**, 229–243.

Mita, K. and Fujiwara, S. (2007). Nodal regulates neural tube formation in the Ciona intestinalis embryo. *Dev. Genes Evol.* **217**, 593–601.

Munro, E. M. and Odell, G. (2002). Morphogenetic pattern formation during ascidian notochord formation is regulative and highly robust. *Development* **129**, 1–12.

Naiche, L. a, Harrelson, Z., Kelly, R. G. and Papaioannou, V. E. (2005). T-box genes in vertebrate development. *Annu. Rev. Genet.* **39**, 219–239.

Nakauchi, M. (1982). Asexual development of ascidians: Its biological significance, diversity, and morphogenesis. *Integr. Comp. Biol.* **22**, 753–763.

Nakauchi, M. and Kawarnura, K. (1978). Additional experiments on the behavior of buds in the ascidian, Aplidium multiplicatum. *Biol. Bull.* **154**, 453–462.

Nardelli, J., Thiesson, D., Fujiwara, Y., Tsai, F. Y. and Orkin, S. H. (1999). Expression and genetic interaction of transcription factors GATA-2 and GATA-3 during development of the mouse central nervous system. *Dev. Biol.* **210**, 305–321.

Niehrs, C., Steinbeisser, H. and De Robertis, E. M. (1994). Mesodermal Patterning by a Gradient of the vertebrate homeobox gene goosecoid. 1–4.

Noda, T. (2011). The maternal genes Ci-p53/p73-a and Ci-p53/p73-b regulate zygotic ZicL expression and notochord differentiation in Ciona intestinalis embryos. *Dev. Biol.* **360**, 216–229.

Nyholm, S. V, Passegue, E., Ludington, W. B., Voskoboynik, A., Mitchel, K., Weissman, I. L. and De Tomaso, A. W. (2006). fester, A candidate allorecognition receptor from a primitive chordate. *Immunity* **25**, 163–73.

Oda-Ishii, I., Bertrand, V., Matsuo, I., Lemaire, P. and Saiga, H. (2005). Making very similar embryos with divergent genomes: conservation of regulatory mechanisms of Otx between the ascidians Halocynthia roretzi and Ciona intestinalis. *Development* **132**, 1663–1674.

Ogasawara, M., Tanaka, K. J., Makabe, K. W. and Satoh, N. (1996). Expression of endostyle-specific genes in the ascidian Halocynthia roretzi. *Dev. Genes Evol.* **206**, 227–

35.

Ogasawara, M., Nakazawa, N., Azumi, K., Yamabe, E., Satoh, N. and Satake, M. (2006). Identification of thirty-four transcripts expressed specifically in hemocytes of Ciona intestinalis and their expression profiles throughout the life cycle. *DNA Res.* **13**, 25–35.

Olsen, C. L., Natzle, J. E. and Jeffery, W. R. (1999). The forkhead gene FH1 is involved in evolutionary modification of the ascidian tadpole larva. *Mech. Dev.* **85**, 49–58.

Papaioannou, V. E. (2014). The T-box gene family: emerging roles in development, stem cells and cancer. *Development* **141**, 3819–3833.

Passamaneck, Y. J., Katikala, L., Perrone, L., Dunn, M. P., Oda-Ishii, I. and Di Gregorio, A. (2009). Direct activation of a notochord cis-regulatory module by Brachyury and FoxA in the ascidian Ciona intestinalis. *Development* **136**, 3679–3689.

Patient, R. K. and McGhee, J. D. (2002). The GATA family (vertebrates and invertebrates). *Curr. Opin. Genet. Dev.* **12**, 416–422.

Ragkousi, K., Beh, J., Sweeney, S., Starobinska, E. and Davidson, B. (2011). A single GATA factor plays discrete, lineage specific roles in ascidian heart development. *Dev. Biol.* **352**, 154–163.

Read, E. M., Rodaway, A. R. F., Neave, B., Brandon, N., Holder, N., Patient, R. K. and Walmsley, M. E. (1998). Evidence for non-axial A/P patterning in the nonneural ectoderm of Xenopus and zebrafish pregastrula embryos. *Int. J. Dev. Biol.* **42**, 763–774.

Rhinn, M., Dierich, a, Shawlot, W., Behringer, R. R., Le Meur, M. and Ang, S. L. (1998). Sequential roles for Otx2 in visceral endoderm and neuroectoderm for forebrain and midbrain induction and specification. *Development* **125**, 845–56.

Rhinn, M., Dierich, a, Le Meur, M. and Ang, S. (1999). Cell autonomous and non-cell

autonomous functions of Otx2 in patterning the rostral brain. *Development* **126**, 4295–304.

Ribeiro, I., Kawakami, Y., Büscher, D., Raya, Á., Rodriguez-León, J., Morita, M., Rodríguez Esteban, C. and Izpisúa Belmonte, J. C. (2007). Tbx2 and Tbx3 regulate the dynamics of cell proliferation during heart remodeling. *PLoS One* **2**,.

Rinkevich, B., Shlemberg, Z. and Fishelson, L. (1995). Whole-body protochordate regeneration from totipotent blood cells. *Proc. Natl. Acad. Sci. U. S. A.* **92**, 7695–7699.

Rothbächer, U., Bertrand, V., Lamy, C. and Lemaire, P. (2007). A combinatorial code of maternal GATA, Ets and beta-catenin-TCF transcription factors specifies and patterns the early ascidian ectoderm. *Development* **134**, 4023–4032.

Roure, A., Lemaire, P. and Darras, S. (2014). An otx/nodal regulatory signature for posterior neural development in ascidians. *PLoS Genet.* **10**, e1004548.

Sabbadin, A. and Zaniolo, G. (1979). Sexual differentiation and germ cell transfer in the colonial ascidianBotryllus schlosseri. *J. Exp. Zool.* **207**, 289–304.

Sabbadin, A., Zaniolo, G. and Majone, F. (1975). Determination of polarity and bilateral asymmetry in palleal and vascular buds of the ascidian Botryllus schlosseri. *Dev. Biol.* **46**, 79–87.

Satoh, N. (1994). *Developmental Biology of Ascidians*. Cambridge .

Sheng, G. and Stern, C. D. (1999). Gata2 and Gata3: novel markers for early embryonic polarity and for non-neural ectoderm in the chick embryo. *Mech. Dev.* **87**, 213–216.

Showell, C., Binder, O. and Conlon, F. L. (2004). T-box genes in early embryogenesis. *Dev. Dyn.* **229**, 201–218.

Simeone, A. (1998). Otx1 and Otx2 in the development and evolution of the mammalian

brain. *EMBO J.* **17**, 6790–6798.

Stolfi, A. and Brown, F. D. (2015). Evolutionary developmental biology of invertebrates 6: Deuterostomia. In *Evolutionary Developmental Biology of Invertebrates 6: Deuterostomia*, pp. 135–204.

Stolfi, a., Wagner, E., Taliaferro, J. M., Chou, S. and Levine, M. (2011). Neural tube patterning by Ephrin, FGF and Notch signaling relays. *Development* **138**, 5429–5439.

Stolfi, A., Lowe, E. K., Racioppi, C., Ristoratore, F., Brown, C. T., Swalla, B. J. and Christiaen, L. (2014). Divergent mechanisms regulate conserved cardiopharyngeal development and gene expression in distantly related ascidians. *Elife* **3**, 1–28.

Tanaka, K. J., Ogasawara, M., Makabe, K. W. and Satoh, N. (1996). Expression of pharyngeal gill-specific genes in the ascidian Halocynthia roretzi. *Dev. Genes Evol.* **206**, 218–26.

Tiozzo, S. and De Tomaso, A. W. (2009). Functional analysis of Pitx during asexual regeneration in a basal chordate. *Evol. Dev.* **11**, 152–62.

Tiozzo, S., Christiaen, L., Deyts, C., Manni, L., Joly, J.-S. and Burighel, P. (2005). Embryonic versus blastogenetic development in the compound ascidian Botryllus schlosseri: insights from Pitx expression patterns. *Dev. Dyn.* **232**, 468–78.

Tiozzo, S., Brown, F. D. and Tomaso, A. W. De (2008a). Regeneration and Stem Cells in Ascidians. 95–112.

Tiozzo, S., Voskoboynik, A., Brown, F. D. and De Tomaso, A. W. (2008b). A conserved role of the VEGF pathway in angiogenesis of an ectodermally-derived vasculature. *Dev. Biol.* **315**, 243–55.

Tokuoka, M., Satoh, N. and Satou, Y. (2005). A bHLH transcription factor gene, Twist-

like1, is essential for the formation of mesodermal tissues of Ciona juveniles. *Dev. Biol.* **288**, 387–396.

Tsarovina, K., Pattyn, A., Stubbusch, J., Müller, F., van der Wees, J., Schneider, C., Brunet, J.-F. and Rohrer, H. (2004). Essential role of Gata transcription factors in sympathetic neuron development. *Development* **131**, 4775–4786.

Vorontsova, M. A. and Liostner, L. D. (1960). *Asexual propagation and regeneration*. (ed. Billet, F (Depatment of Zoology, U. C.) London, New York: Pergamon Press.

Voskoboynik, A., Simon-Blecher, N., Soen, Y., Rinkevich, B., De Tomaso, A. W., Ishizuka, K. J. and Weissman, I. L. (2007). *Striving for normality: whole body regeneration through a series of abnormal generations.*

Wada, S. and Saiga, H. (1999). Cloning and embryonic expression of Hrsna, a snail family gene of the ascidian Halocynthia roretzi: Implication in the origins of mechanisms for mesoderm specification and body axis formation in chordates. *Dev. Growth Differ.* **41**, 9–18.

Wada, S., Katsuyama, Y., Sato, Y., Itoh, C. and Saiga, H. (1996). Hroth an orthodenticle-related homeobox gene of the ascidian, Halocynthia roretzi: its expression and putative roles in the axis formation during embryogenesis. *Mech. Dev.* **60**, 59–71.

Wada, S., Sudou, N. and Saiga, H. (2004). Roles of Hroth, the ascidian otx gene, in the differentiation of the brain (sensory vesicle) and anterior trunk epidermis in the larval development of Halocynthia roretzi. *Mech. Dev.* **121**, 463–74.

Wardle, F. C. and Papaioannou, V. E. (2008). Teasing out T-box targets in early mesoderm. *Curr. Opin. Genet. Dev.* **18**, 418–425.

Watanabe, H. and Newberry, a T. (1976). Budding by oozooids in the polystyelid ascidian

Metandrocarpa tayori Huntsman. *J. Morphol.* **148**, 161–76.

Weston, J. a. and Thiery, J. P. (2015). Pentimento: Neural Crest and the origin of mesectoderm. *Dev. Biol.* **401**, 37–61.

Williams, N. a and Holland, P. W. (1998). Gene and domain duplication in the chordate Otx gene family: insights from amphioxus Otx. *Mol. Biol. Evol.* **15**, 600–7.

Yasuo, H. and Lemaire, P. (2001). Role of Goosecoid, Xnot and Wnt antagonists in the maintenance of the notochord genetic programme in Xenopus gastrulae. *Development* **128**, 3783–93.

Zaniolo, G., Burighel, P. and Martinucci, G. (1986). Ovulation and placentation in Botryllus schlosseri (Ascidiacea): an ultrastructural study. *Can.J.Zool.* **65**, 1181–1190.

Zhou, X. and Vize, P. D. (2004). Proximo-distal specialization of epithelial transport processes within the Xenopus pronephric kidney tubules. *Dev. Biol.* **271**, 322–338.

Supp. Videos: Time-lapse acquisition of a developing embryo of *Botryllus schlosseri*.

V1: 16hrs time-lapse, starting at the end of the 8 cell-stage and until gastrulation.

V2: 16hrs time-lapse, starting at early gastrula and ending at neurula stage.

Embryo diameter = 300 µm

Fig. 1: Blastogenetic cycle of *Botryllus schlosseri*.

(A): General organisation a colony showing adult zooids bearing two primary buds. (B): detail of a primary bud and its budlet at stage C1. (C): stages of the budlet development

(letters in the left bottom corners). A budlet appears as a thickening of the epidermis and the peribranchial chamber leaflet of the primary bud (stage A1), which evaginates into a closed vesicle (stage B2), followed by organogenesis (stages C1-D). The body axes of the primary bud are indicated in black letters, red letters indicate the budlet body axes, when recognizable. Z: zooid; Bud 1: primary bud; b: budlet; amp: ampullae; Oo: oocytes; dashed lines: white = peripheral vasculature, yellow = primary bud, red = budlet; ep: epidermis; hb: haemoblast, iv: inner vesicle; pc: peribranchial chamber; bc: branchial chamber; dt: dorsal tube; gr: gut rudiment; hr: heart rudiment; t: tunic. Scale bar = 150 µm.

Fig. 2: Ectoderm related gene expression in the palleal budlet.

FISH expression patterns of *GATAb* (A-D) and *Otx* (E-H) and their schematic representation (I) during budlet development. Stages are indicated in the left bottom corner. Riboprobes are shown in green, nuclei are counterstained with Hoescht (blue). (A-H): Dotted white lines outline relevant anatomical structures. Arrowhead, if one colour only, represents a discreet signal, if two colours, distinguishes between two distinct anatomical features. Body axes are shown in the right upper corner (in white and black, parental bud axes, in red, budlet axes); (I): *GATAb* and *Otx* are represented in blue and cyan, respectively. Ep: epidermis; iv: inner vesicle; gr: gut rudiment; dt: dorsal tube; bc: branchial chamber; pc: peribranchial chamber; Oo: oocytes; hr: heart rudiment. Red asterisks indicate strong, non-specific signal. Scale bars = 25µm.

Fig. 3: Endoderm related gene expression in the palleal budlet.

FISH expression patterns of *Fox-A1* (A-D) and *GATAa* (E-H) and their schematic representation (I) along budlet development. Stages are indicated in the left bottom corner. Riboprobes are shown in green, nuclei are counterstained with Hoescht (blue). Arrowhead, if one colour only, points a discreet signal, if two colours, distinguishes between two distinct

anatomical features. (A-H): Dotted white lines underline relevant anatomical structures. Body axes are shown in the right upper corner (in white and black, parental bud axes, in red, budlet axes). (I): *Fox-A1* and *GATAa* are represented in light green and dark green, respectively; overlapping expression is purple. Ep: epidermis; iv: inner vesicle; gr: gut rudiment; dt: dorsal tube; bc:branchial chamber; pc: peribranchial chamber; Oo: oocytes; hr: heart rudiment. Red asterisks indicate strong, non-specific signal. Scale bar = 25µm.

Fig. 4: Mesoderm related gene expression in the palleal budlet.

FISH expression patterns of *Gsc* (A-D) and *Tbx2/3* (E-H) and their schematic representation (I) during budlet development. Stages are indicated in the left bottom corner. Riboprobes are shown in green, nuclei are counterstained with Hoescht (blue). White arrowhead in (F) points anterior cells at the dorsal side of the inner vesicle that are not invaginating, but express *Tbx2/3*. (A-H): Dotted white lines underline relevant anatomical structures. Body axes are shown in the right upper corner (in white and black, parental bud axes, in red, budlet axes); (I): *Gsc* and *Tbx2/3* are represented in pink and red, respectively; overlapping expression is in purple. Ep: epidermis; iv: inner vesicle; gr: gut rudiment; dt : dorsal tube; bc: branchial chamber; pc: peribranchial chamber; Oo: oocytes; hr: heart rudiment. Red asterisks indicate strong, non-specific signal. Scale bar = 25µm.

Fig. 5: Induction and characterization of VB.

(A): colony prior dissection; (B): the same colony 48 hours after ablation of all zooids and buds; (C): details of the regenerated zooid bearing palleal buds (red squares), 10 days after surgery. Dashed lines underline the peripheral vasculature. (D-H): details of the onset of VB. (D), (E), (F) and (G): regenerative vascular buds at stage 1, 3, 4 and 5, labelled with Tyrosinated tubulin (green), nuclei are counterstained with Hoescht (blue). Scale bars = 10 µm. H: schematic representation of the vascular bud morphology. Black numbers indicate

arbitrary chosen stages of vascular bud development. Stage 1: compact cell cluster lining on the vessel wall. Stage 2: lumen formation, the vascular bud becomes a hollow vesicle. Stage 3: polarized vascular bud, exhibiting different cell shapes at two opposite sides of the vesicle (cuboidal versus flattened cells). Stage 4: double vesicle stage, where the vascular bud appears as an inner hollow sphere, and the vessel wall forming the outer vesicle. Stage 5: first epithelial folds, and beginning of the non-stereotyped morphogenesis. The last sketch indicates the adult regenerated body (vascular zooid), re-initiating PB (palleal bud in the red square). Amp: ampulla; vb: vascular bud; vw: vessel wall; hb: haemoblast; t: tunic.

Fig. 6: TFs expression in vascular buds.

Gene expression by FISH in vascular buds, before (A-F), and after (G-L) epithelial folds and subsequent organogenesis begins. Gene names are indicated on top of the panel. Riboprobes are shown in green, nuclei are counterstained with Hoescht (blue). Dotted white lines outline the inner epithelia. White arrowhead indicates area(s) of gene expression, note the absence of detection in (A). Presumptive body axes (question mark when unknown) are shown in (G) and (H), based on the identification of several anatomical structures and on resemblance with gene expression during PB. Ve: vascular endothelium; iv: inner vesicle; gr: gut rudiment; bc: branchial chamber; pc: peribranchial chamber. Red asterisks indicate strong, non-specific signal. Scale bar = 30µm.

Fig. 7: *GATAa* Knock-Down.

(A, A'): *GATAa* expression in *GATAa*-siRNA injected colony and in PBS/GFP-siRNA injected control, respectively. (A), the budlet retained the B2 morphology and did not show

morphogenesis, epithelial folds nor *GATAa* expression like in (A'). White arrowhead: expression of *GATAa* in gut rudiment of control colony. White arrow: expected expression in a B2 budlet. (B, B'): morphology (phalloidin, red, and hoescht, blue) of the colony after 6 days of KD. (B), normal adult morphology but there are only 2 instead of 3 generations. (B'): detail of the buds (white square in B), the colony should be in stage A2, here the youngest budlet exhibits a budlet C1 normal morphology: a big central cavity, no epithelial folds nor guts outgrowth, and no sign budding. (C – D'): live pictures of GFP-siRNA (C, C') and *GATAa*-siRNA (D, D') treated colonies. At day 1 of siRNA, colonies are in B1 stage (C, D). At day 5 of treatment (C', D'), the control is in stage D, undergoing apoptosis (C'), while the KD colony shows a delayed development, with contracted (double headed arrows in D') but non-regressing zooids and smaller primary buds than the control. Details of the budlets are shown in the right bottom corners (C' and D'): note the difference in size, morphology and pigmentation. Dashed white line delineates the budlet body. Bc: branchial chamber; gr: gut rudiment; ep: epidermis; iv: inner vesicle; z: zooid; en: endostyle; s: stomach. Scale bar = 30 µm.

Figure 8: Recapitulative scheme of the germ layer markers expression during palleal bud development.

Scheme of TF expression in both primary buds and budlets, at two developmental stages, A2 and B2, from a dorsal view. From left to right: ectoderm-, endoderm- and mesoderm-related TFs. Gene names are indicated in the same colour as their region of expression in the buds. Black lines delineate dorsal-most structures (neural complex, siphons). Dashed black lines delineate ventral-most structures (endostyle, heart and gut rudiments). The expression of *Gsc* in the primary bud dorsal epithelia is not represented. Organ rudiments are indicated on the upper left primary bud only.

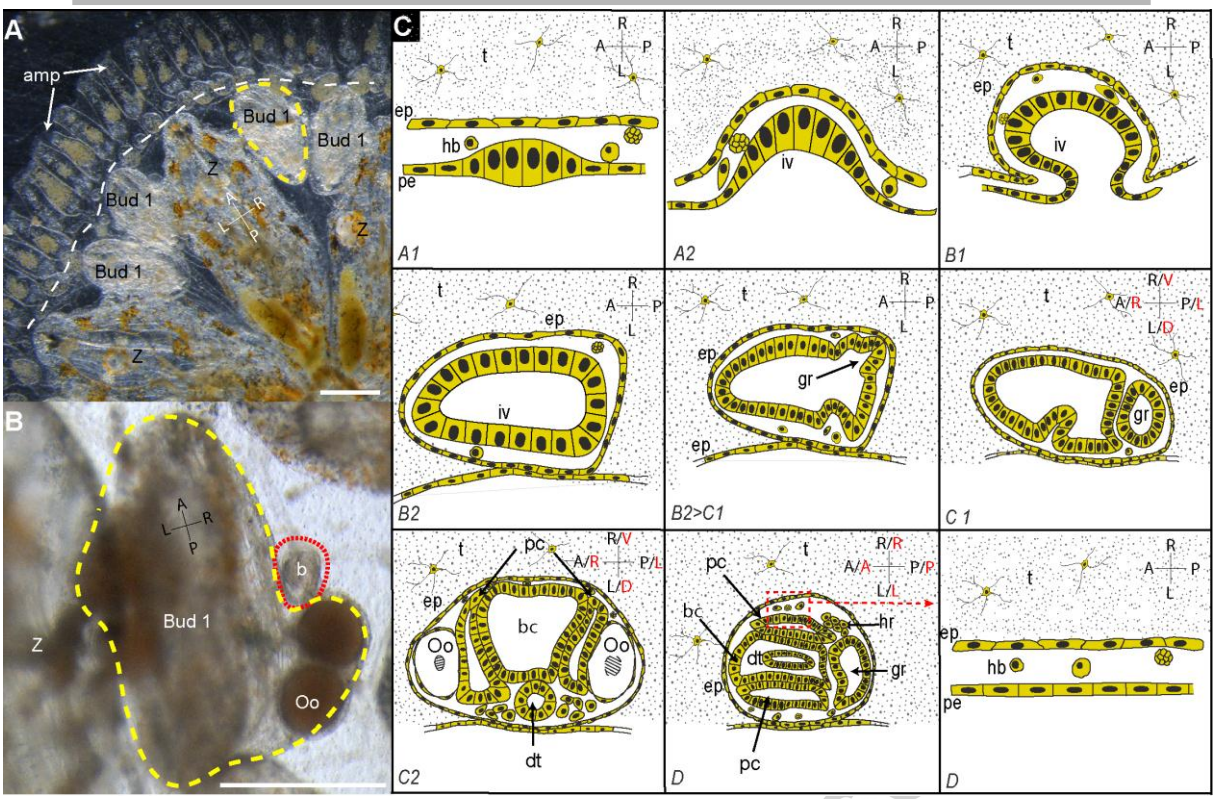

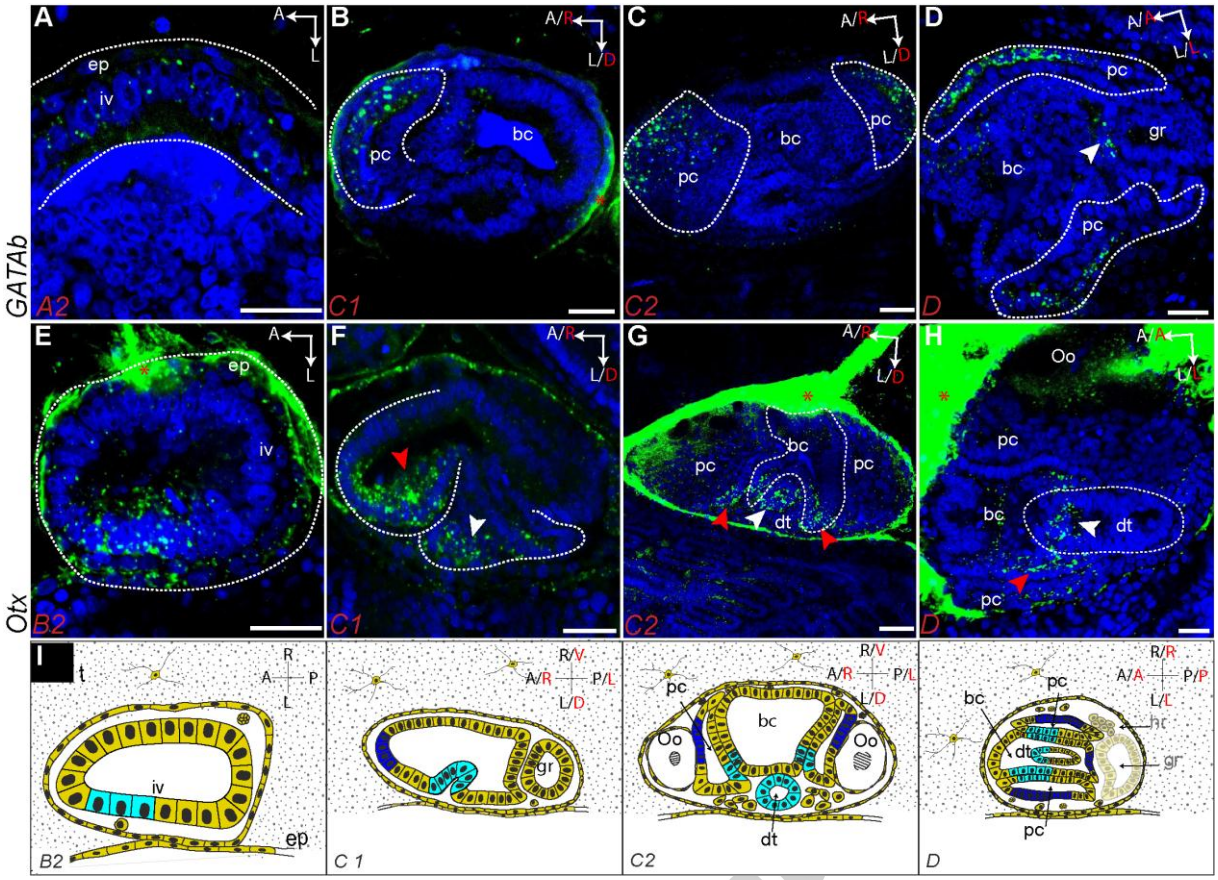

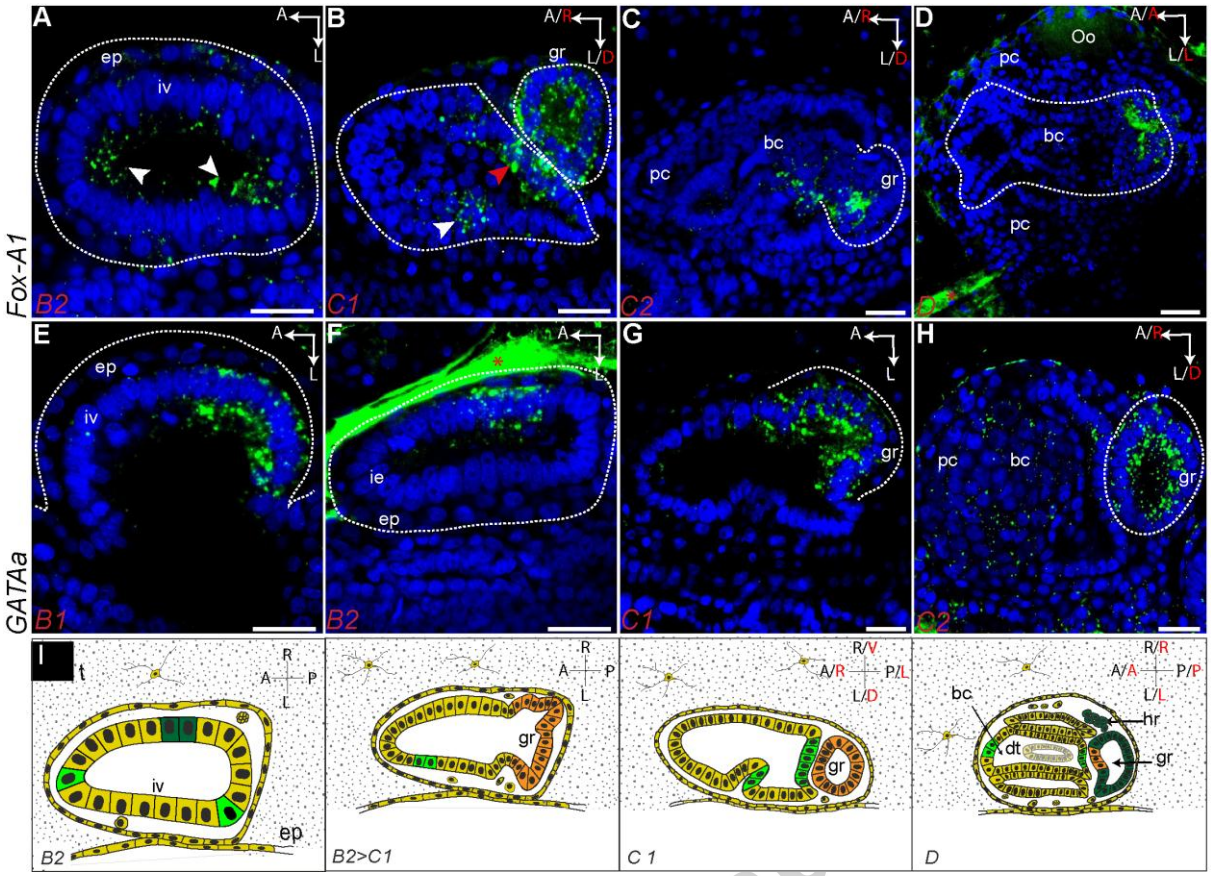

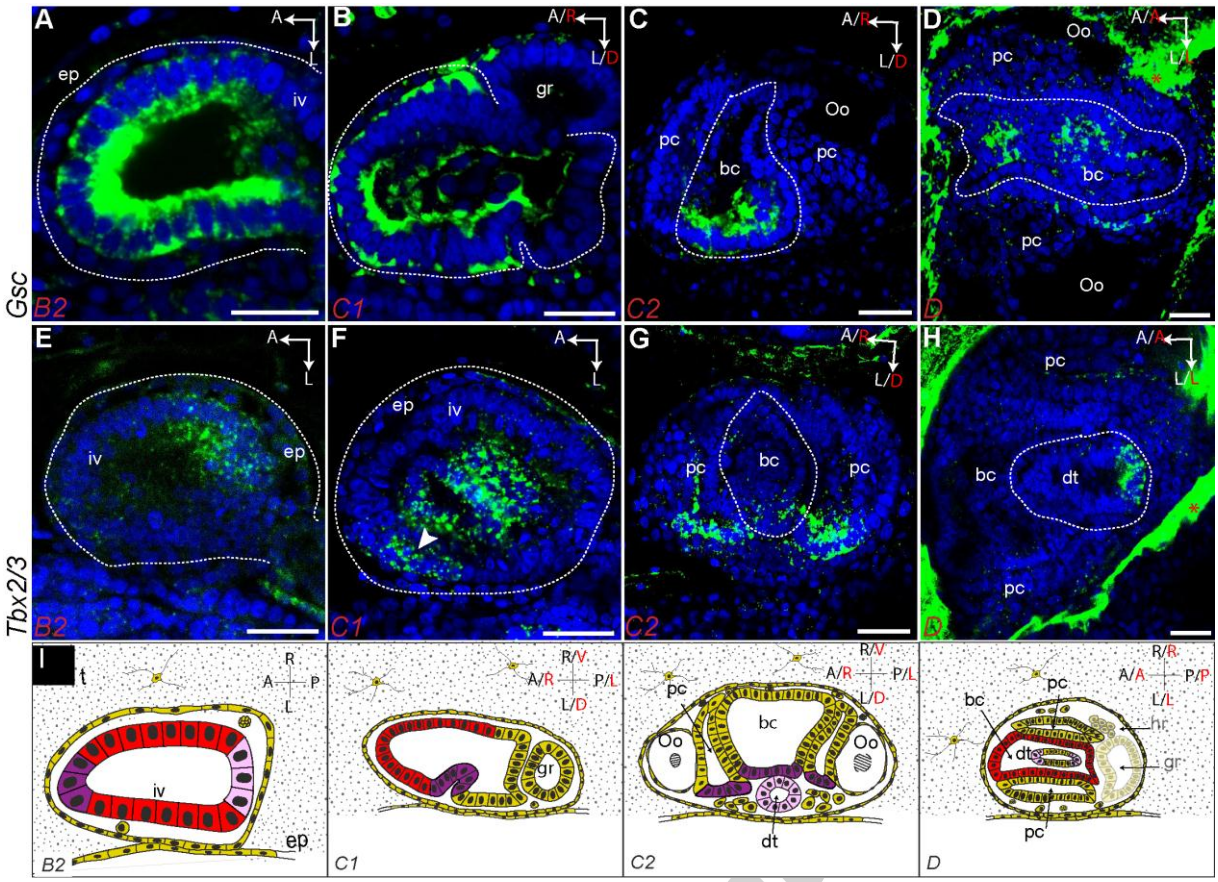

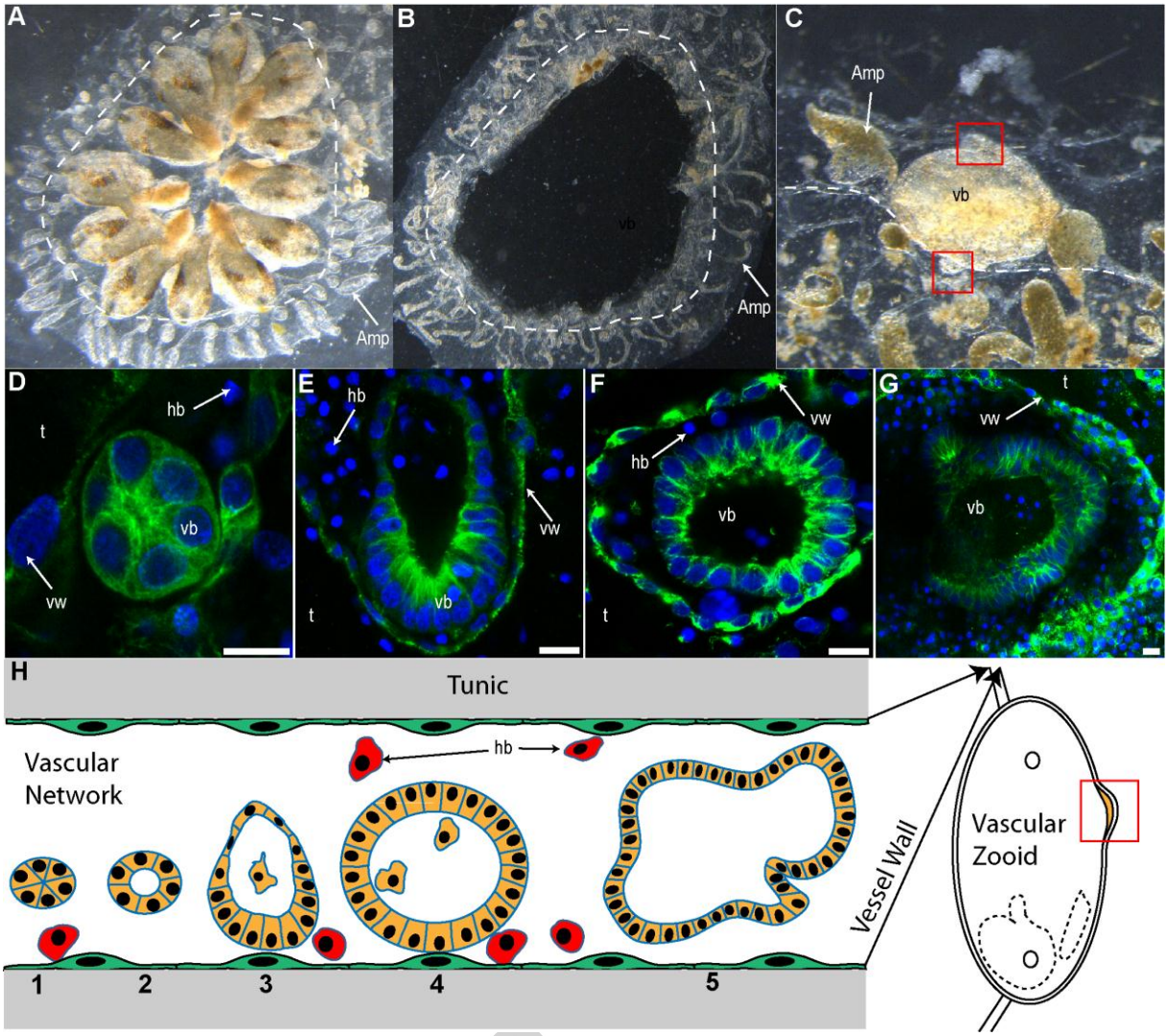

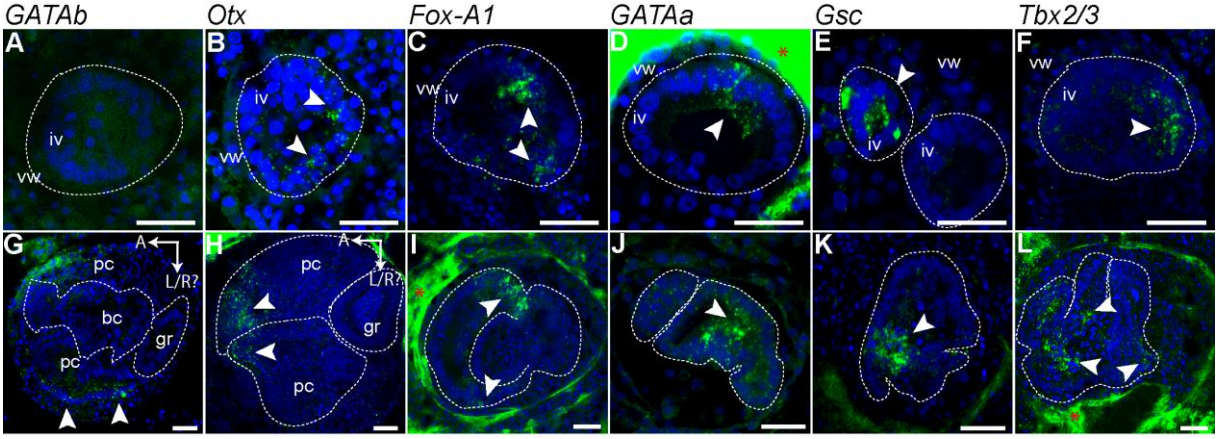

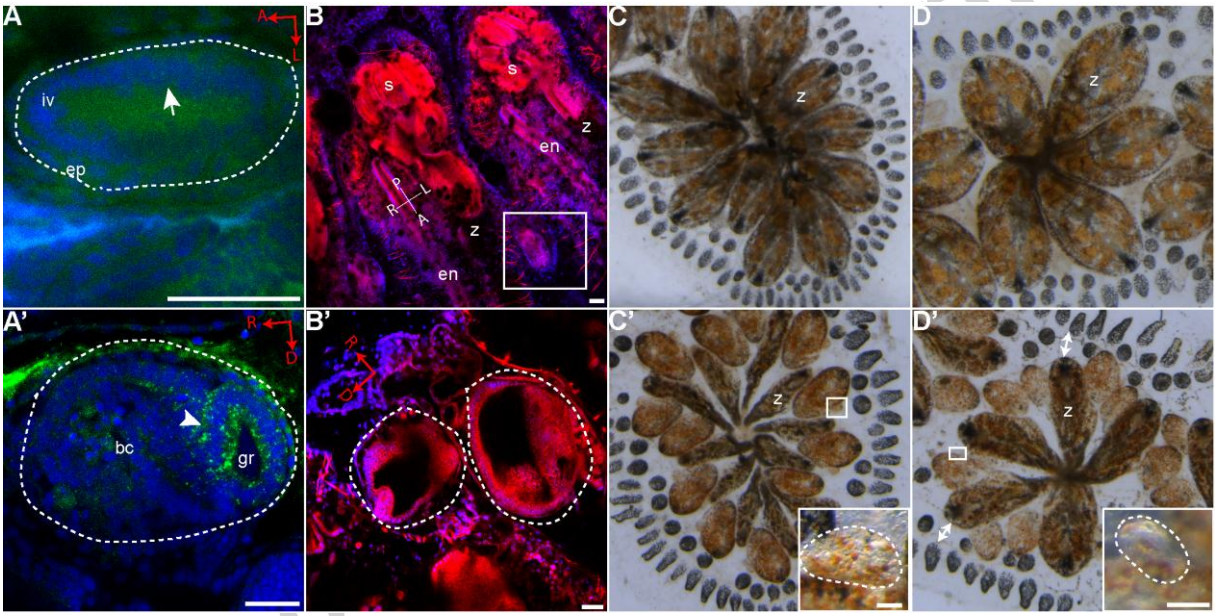

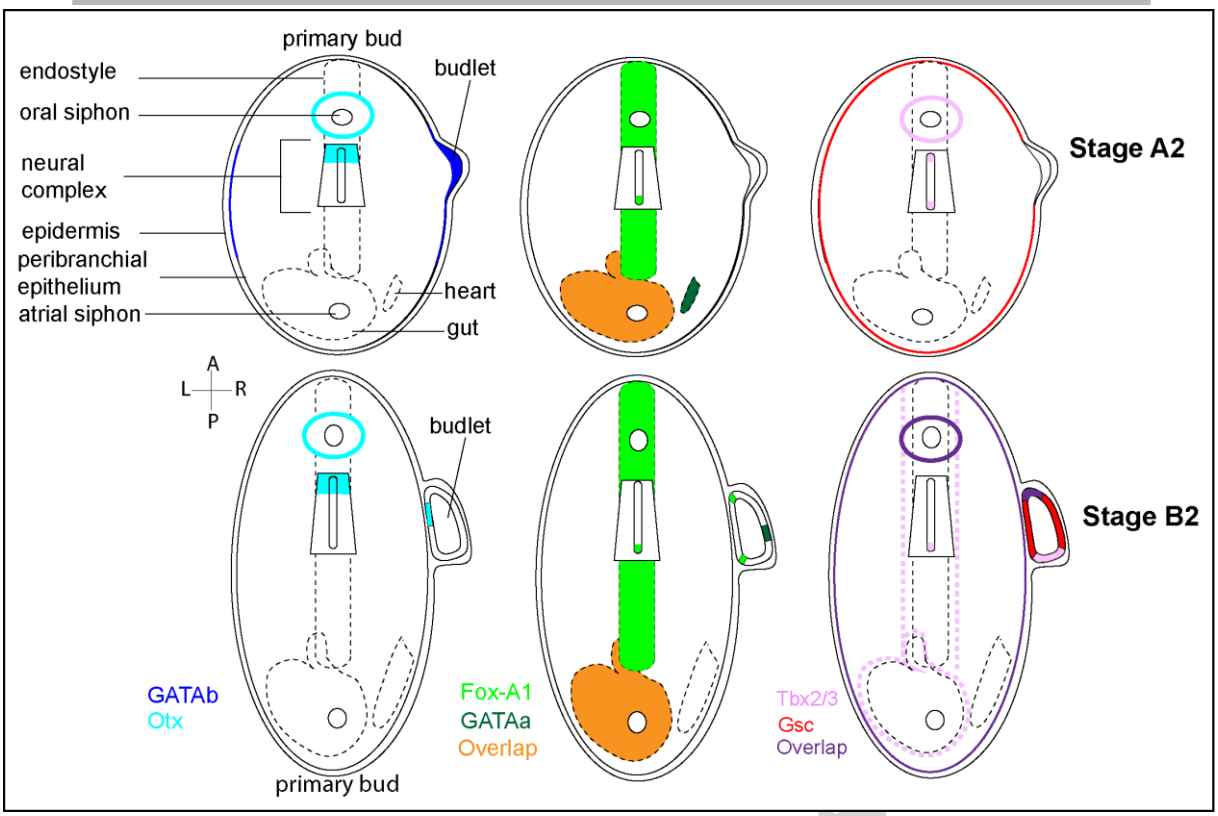

Table 1: Transcription factor expression through palleal bud development

Summary of the presence (+) and absence (-) of expression as observed by FISH. Expression in the adult zooid was either absent or very low compared to expression in palleal buds and budlets, and it was difficult to discern from auto-fluorescence and background noise (+/-).

	Budlet stage				Primary bud stage				Zooid stage			
Gene	A	B	C	D	A	B	C	D	A	B	C	D
Fox-A1	-	+	+	+	+	+	+	+	+/-	+/-	+/-	-
GATA a	-	+	+	+	+	+	+	+	+/-	+/-	+/-	-
Otx	-	+	+	+	+	+	+	-	-	-	-	-
GATA b	+	-	+	+	+	+	-	-	-	-	-	-
Tbx2/3	+	+	+	+	+	+	+	+	-	-	-	-
Gsc	-	+	+	+	+	+	+	+	+/-	+/-	+/-	+/-
Brachyury	-	-	-	-	-	+	+	-	-	-	-	-

Highlights

- Germ layers related TFs are re-used during non-embryonic developments
- Germ layers related TFs show tissue regionalization in blastogenesis and VB
- The regionalization of the TFs suggests an early tissue commitment in PB and VB